

Visualization of Arenavirus RNA Species in Individual Cells by Single-Molecule Fluorescence In Situ Hybridization Suggests a Model of Cyclical Infection and Clearance during Persistence

Benjamin R King, Aubin Samacoits, Philip L Eisenhauer, Christopher M. Ziegler, Emily A Bruce, Daniel Zenklusen, Christophe Zimmer, Florian Mueller, Jason Botten

▶ **To cite this version:**

Benjamin R King, Aubin Samacoits, Philip L Eisenhauer, Christopher M. Ziegler, Emily A Bruce, et al.. Visualization of Arenavirus RNA Species in Individual Cells by Single-Molecule Fluorescence In Situ Hybridization Suggests a Model of Cyclical Infection and Clearance during Persistence. Journal of Virology, 2018, 92 (12), pp.e2241-17. 10.1128/JVI.02241-17 . pasteur-02075021

HAL Id: pasteur-02075021
https://pasteur.hal.science/pasteur-02075021

Submitted on 9 Mar 2020

HAL is a multi-disciplinary open access archive for the deposit and dissemination of scientific research documents, whether they are published or not. The documents may come from teaching and research institutions in France or abroad, or from public or private research centers.

L'archive ouverte pluridisciplinaire **HAL**, est destinée au dépôt et à la diffusion de documents scientifiques de niveau recherche, publiés ou non, émanant des établissements d'enseignement et de recherche français ou étrangers, des laboratoires publics ou privés.

JVI Accepted Manuscript Posted Online 11 April 2018
J. Virol. doi:10.1128/JVI.02241-17
Copyright © 2018 American Society for Microbiology. All Rights Reserved.

Accepted Manuscript Posted Online
Journal of Virology
JVI
Journal of Virology

Downloaded from http://jvi.asm.org/ on March 6, 2020 at NYU LANGONE MED CTR-SCH OF MED

Visualization of arenavirus RNA species in individual cells by single-molecule fluorescence in situ hybridization (smFISH) suggests a model of cyclical infection and clearance during persistence

Benjamin R. King[1,2, §], Aubin Samacoits[3,4], Philip L. Eisenhauer[1], Christopher M. Ziegler[1], Emily A. Bruce[1], Daniel Zenklusen[5], Christophe Zimmer[3,4], Florian Mueller[3,4], and Jason Botten[1,6#]

[1]Department of Medicine, Division of Immunobiology, University of Vermont, Burlington, VT 05405, USA

[2]Cellular, Molecular, and Biomedical Sciences Graduate Program, University of Vermont, Burlington, VT 05405, USA

[3]Unité Imagerie et Modélisation, Institut Pasteur, Paris, France

[4] C3BI, USR 3756 IP CNRS, Paris, France

[5]Departement de Biochimie et Médecine Moléculaire, Université de Montréal, Montréal, QC H3T 1J4, Canada

[6]Department of Microbiology and Molecular Genetics, University of Vermont, Burlington, VT 05405, USA

[§]Current address: Institute for Systems Genetics, New York University School of Medicine, New York, NY, 10016, USA

#Corresponding author

E-mail: jbotten@uvm.edu

Accepted Manuscript Posted Online

Journal of Virology

JVI

Journal of Virology

22 **Running Title:** Cyclical LCMV infection and clearance in persistence

23 **Word count (Abstract):** 250

24 **Word count (text):** 6,781

Downloaded from http://jvi.asm.org/ on March 6, 2020 at NYU LANGONE MED CTR-SCH OF MED

Accepted Manuscript Posted Online

ABSTRACT

Lymphocytic choriomeningitis mammarenvirus (LCMV) is an enveloped, negative-strand RNA virus that causes serious disease in humans but establishes an asymptomatic, lifelong infection in reservoir rodents. Different models have been proposed to describe how arenaviruses regulate the replication and transcription of their bisegmented, single-stranded RNA genomes, particularly during persistent infection. However, these models were largely based on viral RNA profiling data derived from entire populations of cells. To better understand LCMV replication and transcription at the single-cell level, we established a high-throughput, single-molecule (sm)FISH image acquisition and analysis pipeline and examined viral RNA species at discrete time points from viral entry through the late stages of persistent infection *in vitro*. We observed transcription of viral nucleoprotein and polymerase mRNAs from the incoming S and L segment genomic RNAs, respectively, within 1 hr of infection, whereas transcription of glycoprotein mRNA from the S segment antigenome required ~4-6 hr. This confirms the temporal separation of viral gene expression expected due to the ambisense coding strategy of arenaviruses and also suggests that antigenomic RNA contained in virions is not transcriptionally active upon entry. Viral replication and transcription peaked at 36 hours post-infection, followed by a progressive loss of viral RNAs over the next several days. During persistence, the majority of cells showed repeating cyclical waves of viral transcription and replication followed by clearance of viral RNA. Thus, our data support a model of LCMV persistence whereby infected cells can spontaneously clear infection and become reinfected by viral reservoir cells that remain in the population.

Downloaded from http://jvi.asm.org/ on March 6, 2020 at NYU LANGONE MED CTR-SCH OF MED

Journal of Virology JVI Journal of Virology

Accepted Manuscript Posted Online

Journal of Virology

JVI

Journal of Virology

Downloaded from http://jvi.asm.org/ on March 6, 2020 at NYU LANGONE MED CTR-SCH OF MED

IMPORTANCE

Arenaviruses are human pathogens that can establish asymptomatic, life-long infections in their rodent reservoirs. Several models have been proposed to explain how arenavirus spread is restricted within host rodents, including the periodic accumulation and loss of replication competent, but transcriptionally incompetent, viral genomes. A limitation of previous studies was the inability to enumerate viral RNA species at the single cell level. We developed a high throughput, single-molecule RNA (sm)FISH assay and used it to quantitate lymphocytic choriomeningitis mammarenavirus (LCMV) replicative and transcriptional RNA species in individual cells at distinct time points following infection. Our findings support a model whereby productively infected cells can clear infection, including viral RNAs and antigen, and later be reinfected. This information improves our understanding of the timing and possible regulation of LCMV genome replication and transcription during infection. Importantly, the smFISH assay and data analysis pipeline developed here is easily adaptable to other RNA viruses.

INTRODUCTION

Several members of the arenavirus family are significant threats to human health. Lassa virus and Junín virus cause hemorrhagic fever syndromes while lymphocytic choriomeningitis virus (LCMV), the prototypic member of the family, is a well-known cause of severe birth defects and is highly lethal in immunocompromised individuals (1, 2). A critical imperative to better understand the key steps of the arenavirus life cycle is made evident by the fact that there are no FDA-approved vaccines to prevent arenavirus transmission and only a very limited repertoire of

Accepted Manuscript Posted Online

Journal of Virology

JVI

Journal of Virology

Downloaded from http://jvi.asm.org/ on March 6, 2020 at NYU LANGONE MED CTR-SCH OF MED

69 antivirals (3, 4). New strategies to prevent and treat arenavirus infections will likely hinge upon
70 an improved understanding of key phases of the life cycle of these important human pathogens.

71 Arenaviruses are enveloped viruses that have a single-stranded, bisegmented, negative-
72 sense RNA genome. The ~3.5 kb small (S) and ~7.2 kb large (L) genomic RNA segments each
73 encode two viral open reading frames in ambisense orientation (Fig. 1A) (1). The nucleoprotein
74 (NP) and polymerase (L) genes are encoded in typical negative-sense orientation on genomic
75 RNA while the glycoprotein (GPC) and matrix protein (Z) genes are encoded in pseudo positive-
76 sense orientation. The canonical sequence of genetic events following the release of arenavirus
77 genomic RNA into the cytoplasm of a newly infected cell is (i) primary transcription of the NP
78 and L mRNAs from the viral S and L genomic segments, respectively, followed by (ii) full
79 length replication of the S and L segment antigenomic RNAs and subsequent transcription of the
80 GPC and Z mRNAs from the S and L antigenomic RNAs, respectively, and (iv) replication of
81 additional full-length genomic RNAs from the antigenomic RNA templates (Fig. 1A) (1, 5).

82 While rodent-borne arenaviruses cause severe diseases in humans, they are thought to be
83 asymptomatic in their sylvatic hosts, where they can establish a persistent, life-long infection (1).
84 LCMV is carried by the common house mouse and can be transmitted vertically from mother to
85 pup (6-8). The pups are born infected but never mount an effective immune response to clear the
86 virus as viral proteins are seen as self-antigens by the pup's developing immune system (6-8) .
87 Paradoxically, while LCMV can infect most cells in the host rodent, it tightly regulates its spread
88 and therefore does not overrun its host. Several hypotheses have been proposed for how LCMV
89 restricts its spread, including through (i) the production of defective interfering (DI) particles (9-
90 11), which can enter susceptible host cells and make them refractory to productive infection (12,
91 13) and (ii) the accumulation of transcriptionally-defective genomic and antigenomic RNAs,

Accepted Manuscript Posted Online

Journal of Virology

JVI

Journal of Virology

Downloaded from http://jvi.asm.org/ on March 6, 2020 at NYU LANGONE MED CTR-SCH OF MED

which limit viral protein expression and infectious virus production (5, 14, 15). It has also been proposed that LCMV can establish a cyclical, transient pattern of infection such that susceptible cells are productively infected for a short time before clearing the virus and once again becoming susceptible to reinfection by neighboring cells that remain productively infected (16-19).

A current gap in our knowledge of how arenaviruses restrict their dissemination is that we lack a detailed understanding of how the events of viral genome replication and transcription are regulated during the acute and persistent phases of infection. Previous studies examining the genetic events of arenavirus replication and transcription, including those described above regarding the accumulation of transcriptionally defective RNAs (5, 14, 15), relied on techniques such as Northern blot or quantititative RT-PCR. Both are powerful techniques used to examine RNA. Quantitative RT-PCR is exquisitely sensitive (20), and Northern blot is able to specifically distinguish between each of the viral RNA species (15, 21-29). However, both techniques measure RNA at a population level and thus provide population average data. Variability in RNA expression between individual cells in a heterogeneous population cannot be evaluated using these approaches. Single-molecule RNA fluorescence in situ hybridization (smFISH) can bridge this technical gap to allow for detection of RNAs with single-copy sensitivity in individual cells by fluorescence microscopy (30). In the present study, we designed specific smFISH probe sets to fluorescently-label different LCMV RNA species (Fig. 1A) and to quantitatively characterize their expression in single cells at discrete time points throughout the acute and persistent phases of arenavirus infection in an *in vitro* model. Our studies confirm the temporal separation of LCMV negative-sense and pseudo positive-sense gene expression and show a pattern of cyclical loss and reappearance of viral RNA in most cells during persistence in a cell culture model of infection. Our studies provide insight into the functional genetic

Accepted Manuscript Posted Online

Journal of Virology

JVI

Journal of Virology

Downloaded from http://jvi.asm.org/ on March 6, 2020 at NYU LANGONE MED CTR-SCH OF MED

115 composition of infectious virions, the kinetics of transcription and replication in the hours
116 immediately following initial infection, and support a model of cyclical viral replication and
117 transcription during persistence. Further, the image acquisition and analysis pipeline developed
118 here is easily adaptable to other viruses.

119

120 **RESULTS**

121 **Visualization of LCMV RNA species in infected cells.** To visualize LCMV RNAs in
122 cells by fluorescence microscopy, we designed smFISH probe sets complementary to different
123 viral RNA species (see overview in Fig. 1A). An important feature of smRNA FISH is the ability
124 to detect single RNA molecules using multiple, singly-labeled oligonucleotide probes (30). The
125 probe set binding to a specific target RNA causes single RNAs to appear as bright spots. To
126 validate our ability to specifically label arenavirus RNAs, we used a cellular mRNA smFISH
127 probe set specific for the housekeeping gene MDN1 as a control (Fig. 1B) for comparison with a
128 smFISH probe set designed to target both the viral S genome RNA and GPC mRNA (Fig. 1C).
129 MDN1 probes detect cytoplasmic mRNAs as well as sites of active transcription in the nucleus
130 (Fig. 1B). Next, we confirmed that the viral RNA smFISH probe set is highly specific as
131 fluorescent signal was absent in uninfected cells, but bright spots were detected in LCMV-
132 infected cells fixed at 24 hpi (Fig. 1C). Moreover, similar to smFISH staining obtained with our
133 control MDN1, individual smFISH spots were homogeneous in size, shape, and fluorescence
134 intensity (Fig. 1B and C) consistent with the detection of single RNAs, as shown previously (30,
135 31). Furthermore, in contrast to the nuclear transcribed MDN1 mRNAs, viral RNAs were largely
136 excluded from the nucleus, consistent with the cytoplasmic viral life cycle (Fig. 1B to C).

Accepted Manuscript Posted Online

Journal of Virology

JVI

Journal of Virology

Downloaded from http://jvi.asm.org/ on March 6, 2020 at NYU LANGONE MED CTR-SCH OF MED

smFISH probes complementary to viral mRNA species provide high signal-to-noise staining. We designed multiple smFISH probe sets to have specificity for different RNA species produced during the course of the LCMV life cycle (Fig. 1A). Specifically, these probe sets target (i) S genome only, (ii) GPC mRNA and S genome, (iii) NP mRNA and S antigenome, or (iv) L mRNA and L antigenome. When infected cells were stained with probe sets complementary to "S genome and GPC mRNA" (referred to as "GPC mRNA/S genome" from this point forward), we noted high quality staining with the GPC mRNA/S genome probes as evidenced by homogeneity in spot size, shape, and intensity (Fig. 2A) and high signal-to-noise ratio (Fig. 3). The NP mRNA/S antigenome and L mRNA/L antigenome probe sets yielded similar high quality staining as evidenced by high signal-to-noise ratios (Fig. 3). However, we noted lower quality staining with the "S genome only" probes as evidenced by the dimmer staining (Fig. 2) and low signal-to-noise ratio (Fig. 3). Moreover, the "S genome only" probes yielded greater non-specific staining in uninfected cells, potentially leading to detection of false-positive spurious events (Fig. 2C) – perhaps an artifact of the long exposure times and high light intensity needed to detect this less sensitive probe set binding to its target. Similarly low signal-to-noise ratios were observed with probe sets specific for "S antigenome only" or "L genome only" (data not shown). It is possible that the encapsidation of genome and antigenome by viral nucleoprotein partially occludes smFISH probe hybridization with these target RNA sequences and thus leads to the lower signal-to-noise ratio observed with these probe sets. Therefore, use of these probe sets with cells containing small numbers of viral RNAs would be problematic due to the level of background staining observed (Fig. 2C). However, these probe sets are effective when paired with cells containing abundant copies of viral genome or antigenome (Fig. 2B and data not shown) (32), which easily exceeds the quantity of background spots observed in mock-

Accepted Manuscript Posted Online

Journal of Virology

JVI

Journal of Virology

Downloaded from http://jvi.asm.org/ on March 6, 2020 at NYU LANGONE MED CTR-SCH OF MED

160 infected control cells (Fig. 2C). Because the probe sets that targeted an mRNA plus either
161 genome or antigenome provided the highest quality staining and sensitivity, we elected to use
162 these probe sets to follow the kinetics of viral transcription and replication events in infected
163 cells.

164 **smFISH spot detection and quantification in individual LCMV-infected cells.** A
165 primary goal of our study was to globally describe the kinetics of transcription and replication of
166 the LCMV genome from the early hours following viral entry through the late stages of
167 persistence. Ideally, we would be able to infect cells at a high multiplicity of infection (MOI) and
168 take snapshots of a population of synchronously infected cells at time points throughout the
169 entire course of arenavirus infection. However, we were obliged to infect cells at a low MOI due
170 to the characteristic high prevalence of DI particles present in LCMV stocks (33). Because only a
171 small proportion of cells would be productively infected upon viral inoculation, we needed to
172 image a large population of cells at each time point tested to provide an accurate portrait of the
173 heterogeneity present in a population of asynchronously infected cells. Thus, it was important for
174 this study to both image and quantitatively characterize the smFISH staining of viral RNAs in a
175 high-throughput fashion. To accomplish this goal, we automatically segmented the nuclei using
176 DAPI and cell outlines using CellMask Green fluorescent staining with CellProfiler software
177 (34) (Fig. 4A). Next, smFISH-labeled viral RNAs were detected using FISH-quant software (35)
178 (Fig. 4B). We were able to image two distinct RNA smFISH probe sets labeled with spectrally-
179 distinct fluorophores in individual cells. This allowed us to characterize relative viral RNA
180 expression levels and compare localization of different viral RNAs (Figs. 4B to C). We were
181 able to robustly quantify viral RNAs using FISH-quant across a range of expression levels. We
182 observed a direct relationship between the number of detected spots and the total fluorescence

Accepted Manuscript Posted Online

Journal of Virology

JVI

Journal of Virology

Downloaded from http://jvi.asm.org/ on March 6, 2020 at NYU LANGONE MED CTR-SCH OF MED

signal in the smFISH channel up to approximately 1,000 RNAs/cell, after which the number of detected viral RNAs reached a plateau (Fig. 4D). This represents the point at which smFISH spots are so dense, that we were no longer able to accurately distinguish closely spaced RNAs. Examples of a cell displaying moderate levels of viral RNAs where identification of diffraction limited spots was robust (Fig. 4B) and a cell with very high expression of viral RNAs where overcrowded spots are unable to be effectively spatially resolved (Fig. 4C) are shown for reference. Thus, when viral RNA levels are relatively low (less than a thousand copies per cell) we have high confidence in the accuracy of the quantification provided by FISH-quant. However, when viral RNA levels are at their peak and RNAs are very dense, quantification is an underestimate of RNA expression levels and may complicate our ability to assess relative levels of different RNA species when both are expressed at high levels.

Viral RNA transcription and replication following viral entry. We next aimed to monitor the early events of viral genomic transcription and replication immediately following viral entry. Cells were infected with LCMV at an MOI of 0.1, fixed at multiple time points, stained for NP mRNA/S antigenome, GPC mRNA/S genome, or L mRNA/L antigenome, and several hundred cells were imaged and analyzed at each time point. As discussed above in relation to Fig. 2, our probes sets specific for only genome or antigenome (but not an additional complementary viral mRNA) have low signal-to-noise ratios and sensitivity when compared to probe sets that also target a viral mRNA. Importantly, FISH-quant was unable to detect viral genome or antigenome spots in cells that had been infected with LCMV for less than 8 h (Fig. 2 and data not shown). However, by 8 hpi and later, genome and antigenome spots become detectable with these probe sets (Fig. 2) (32). Therefore, in this set of experiments, smFISH spots detected with the NP mRNA/S antigenome, GPC mRNA/S genome, or L mRNA/L antigenome

Accepted Manuscript Posted Online

Journal of Virology

JVI

Journal of Virology

Downloaded from http://jvi.asm.org/ on March 6, 2020 at NYU LANGONE MED CTR-SCH OF MED

probe sets prior to 8 hpi are presumed to represent only the designated mRNA target in each case, whereas at 8 hpi and later it is possible to detect a mixture of the targeted RNAs.

Representative images of cells infected from 0 to 6 hpi are shown (Fig. 5A to B). Notably, transcription of the NP mRNA and L mRNA is detected as early as 1 hour following infection (Fig. 5 and 6A to B) indicating primary transcription of the S and L genomic RNA occurs soon after entry and uncoating of arenavirus virions. The GPC mRNA, on the other hand, is first detected at 6 hours following infection (Fig. 5A and 6A and C). This delayed appearance of the GPC mRNA suggests that transcriptionally competent S antigenomic RNA is not delivered into cells by incoming virions. Further, it suggests that a 4-6 hour lag is required for the production of S antigenomic RNA, which serves as the template for transcription of GPC mRNA (Fig. 1A). This result is in agreement with previous studies that examined arenavirus mRNA synthesis via Northern blot (5, 26).

When examining the subcellular localization of NP mRNA and GPC mRNA or NP mRNA and L mRNA pairs at 6 hpi or earlier, no overt colocalization between viral mRNAs was noted (Fig. 5A to B).

Disproportionate transcription of S segment genes early after infection. For each probe set used in the experiments shown in Figs. 5 and 6, the number of false-positive viral RNAs detected in mock-infected cells was used to establish a threshold to classify cells as either "positive" or "negative" for each of the tested viral RNA species. At 6 hpi (a time point before virus in the initially infected cells could have completed its life cycle and spread to adjacent, initially uninfected cells (36-39), we observed that 65-90% of cells were positive for NP mRNA and 40% were positive for GPC mRNA (Fig. 6C to D). This high frequency of cells containing S segment-derived transcripts was surprising given the fact we initially infected cells at an MOI of

Accepted Manuscript Posted Online

Journal of Virology

JVI

Journal of Virology

Downloaded from http://jvi.asm.org/ on March 6, 2020 at NYU LANGONE MED CTR-SCH OF MED

229 0.1, and thus would have expected approximately only 10% of cells to have been expressing
230 viral RNAs at this early time point. However, at this same early time point, only 8% of cells
231 were positive for L segment-derived L mRNA (Fig. 6D), which is consistent with the expected
232 frequency of viral RNA-positive cells based on the initial MOI. This result may suggest that a
233 high proportion of viral particles either fail to package the L genome or alternatively deliver a
234 transcriptionally-defective L genome.

235 **Viral RNA replication and transcription at peak of acute infection.** To profile LCMV
236 RNAs at the peak of infectious virus release during acute infection, cells were infected with
237 LCMV at an MOI of 0.01, fixed at various time points between 12 and 96 hpi, stained for NP
238 mRNA/S antigenome, GPC mRNA/S genome, or L mRNA/L antigenome, and several hundred
239 cells were imaged and analyzed at each time point. Levels of viral RNAs detected by each probe
240 set rapidly increased over the first 24 hours of infection (Fig. 7A to B and 8A to B). The
241 proportion of cells positive for these viral RNAs also rapidly increased over the first 24 hours of
242 infection such that almost all cells had substantial levels of all viral RNAs (Fig. 8C to D). Peak
243 viral transcription and replication occurred at 36 hours post infection (Fig. 7A to B and 8A to B).
244 At this time point, viral smFISH signal was very dense and true levels of viral NP mRNA and
245 GPC mRNA were likely underestimated due to inability of FISH-quant to accurately count
246 tightly packed viral RNAs in the cytoplasm of infected cells (Fig. 4B to C, 7A to B, and 8A to
247 B). Nevertheless, it is clear that RNAs detected by the S segment-specific probe sets greatly
248 exceeded those detected by the L segment-specific probe set (at least 10-35 fold greater) between
249 12 and 96 hpi (Fig. 8A to B, Table 1). Following peak viral transcription and replication at 36
250 hours post-infection, levels of viral RNAs began to decrease (Fig. 7A to B and 8A to B). The
251 proportion of cells positive for L mRNA/L antigenome expression decreased steadily beginning

Accepted Manuscript Posted Online

Journal of Virology

JVI

Journal of Virology

Downloaded from http://jvi.asm.org/ on March 6, 2020 at NYU LANGONE MED CTR-SCH OF MED

252 at 48 hours post-infection (Fig. 8D). In contrast, all cells maintained NP mRNA/S antigenome
253 and GPC mRNA/S expression over this entire time period (Fig. 8C to D).

254 **Cyclical patterns of infectious virus production and antigen expression during**
255 **persistent infection.** A key feature of arenavirus infection in cell culture is the cyclical pattern of
256 infectious virus release observed during the persistent phase of infection (16, 19, 40-42). We
257 were particularly interested in using smFISH to assess how viral gene expression programs
258 change during persistence and to examine how this correlated with production of infectious virus
259 and translation of viral antigens. Toward this goal, cells were infected with LCMV at an MOI of
260 0.01, supernatants were collected and cells were fixed at multiple time points between 1.5 and 30
261 days (d)pi. As shown in Fig. 9A, A549 cells persistently infected with LCMV cyclically released
262 waves of infectious virus over the first 30 days (Fig. 9A). We were curious how much viral
263 antigen and viral RNA would be expressed in persistently infected cells at time points when cells
264 were releasing high levels of infectious viral particles but also how much viral material was
265 expressed at time points when cells released very little infectious virus. Therefore, we performed
266 IFA to visualize NP or GPC and smFISH to visualize NP mRNA/S antigenome and GPC
267 mRNA/S in cells at multiple time points that corresponded to high and low points in infectious
268 viral release (Fig. 9B to C). At 1.5 (d)pi, all cells expressed NP and GPC protein (Fig. 9B to C).
269 Viral antigen expression mirrored the cycles of infectious virus release as seen in Fig. 9A. Viral
270 antigen was expressed in fewer cells and/or at lower levels at 8 and 27 (d)pi (time points with
271 low levels of infectious viral release) compared to 13 and 30 (d)pi (time points with higher levels
272 of infectious viral release) (Fig. 9B to C). While our goal was to visualize both viral RNA and
273 viral antigen in infected cells by fluorescence microscopy, the sensitivity of smFISH was greatly
274 reduced when combined with IFA – as evidenced by higher levels of background and lower

Accepted Manuscript Posted Online

Journal of Virology

JVI

Journal of Virology

Downloaded from http://jvi.asm.org/ on March 6, 2020 at NYU LANGONE MED CTR-SCH OF MED

signal intensity (Fig. 9B to C). However, taking into account the lower sensitivity of smFISH in this particular experiment, we did see a correlation between the presence of viral RNA within cells and the expression of viral proteins (Fig. 9B to C). Thus, these results suggest that cells infected with LCMV can clear the infection as evidenced by the majority of cells at specific time points (e.g. 8 and 27 dpi) that lack viral RNA or protein and produce little infectious virus.

Cyclical patterns of genome transcription and replication during persistent infection. As smFISH sensitivity in our hands is diminished when performed in conjunction with immunofluorescent staining, we next used smFISH alone to examine the transcription and replication dynamics of arenavirus genomic RNA during the persistent phase of infection at the level of individual RNA molecules. Cells were infected with LCMV at an MOI of 0.01, fixed at multiple time points between 1.5 and 41 days (d)pi, stained for NP mRNA/S antigenome, GPC mRNA/S genome, or L mRNA/L antigenome, and several hundred cells were imaged and analyzed at each time point. Note that our smFISH assay does not allow us to follow particular cells over time, but instead to capture the viral RNA signature of individual cells at specific time points during infection. Following peak RNA transcription and replication at 36 hpi, we observed decreased levels of NP mRNA/S antigenome, GPC mRNA/S genome, or L mRNA/L antigenome over the next several days such that at 8 dpi, the majority of cells examined were negative for all of these viral RNAs (Fig. 10A to F). However, by 13 dpi, the levels of viral RNAs detected by each probe set were increased and the majority of cells were again positive for all viral RNAs (Fig. 10C and F). Viral RNA levels again dropped and many cells were no longer positive for viral RNA by 16 dpi. (Fig. 10C and F). This pattern of viral RNA clearance followed by increased levels of viral RNA expression and increased frequency of viral RNA expressing cells in the population repeated in a cyclical fashion multiple times over the first 41 days

Accepted Manuscript Posted Online

Journal of Virology

JVI

Journal of Virology

Downloaded from http://jvi.asm.org/ on March 6, 2020 at NYU LANGONE MED CTR-SCH OF MED

following infection (Fig. 10). In summary, the sequential loss and reappearance of viral gene expression observed in these studies may represent a genetic signature of the previously recognized phenomenon of cyclical production of infectious LCMV virions over time in cell culture models of persistent infection (16-18).

Throughout the time course of persistence examined in this study, NP mRNA/S antigenome was generally expressed at higher levels than GPC mRNA/S genome (up to 5-fold higher levels) (Fig. 10B and Table 1). The ratio between levels of NP mRNA/S antigenome and L mRNA/L antigenome over this time period was more variable. At time points such as 13 and 20 dpi, when most cells in the culture are positively expressing all viral RNA species, NP mRNA/S antigenome greatly outnumbered L mRNA/L antigenome (~25-fold higher levels) (Fig. 10E and Table 1). However, at other times such as 8, 16, 27, and 34 dpi, when substantial proportions of cells had lost expression of one or more viral RNAs, the ratio between NP mRNA/S antigenome and L mRNA/L antigenome in the double-positive cells was greatly reduced (~2-fold higher levels of NP than L mRNA) (Fig. 10E and Table 1). Notably, the magnitude of viral RNA expression during persistence never reached the high levels observed at the peak of acute infection (Fig. 10).

DISCUSSION

In the current study, we developed a high throughput smFISH assay that allowed us to visualize single copies of LCMV RNAs in individual cells. Taking advantage of the sensitivity and quantitative aspect of this assay, we tracked the dynamics of viral replication and transcription spanning early time points following initial virus entry to late times during

Accepted Manuscript Posted Online

Journal of Virology

JVI

Journal of Virology

Downloaded from http://jvi.asm.org/ on March 6, 2020 at NYU LANGONE MED CTR-SCH OF MED

persistent infection. We observed that transcription of the negative-sense encoded NP and L mRNAs precede that of the pseudo positive-sense encoded GPC mRNA, confirming the temporal separation of gene expression predicted by the ambisense coding strategy of the arenaviruses and suggesting that antigenomic RNA in virions is not transcriptionally active following release into a newly infected cell. Our studies demonstrated a hierarchal pattern of expression among viral RNAs and indicate that many infecting virus particles may lack L genomic RNA. Finally, over the course of persistent infection, we observed repeated cycles whereby cells appeared to transition from supporting active viral replication and transcription to a state where viral RNA is undetectable by smFISH. Collectively, these studies improve our understanding of the natural history of arenavirus replication and transcription during acute and persistent infection.

The smFISH assay developed here provided us with an opportunity to build upon prior studies and examine arenavirus genome replication and transcription with greater sensitivity and detail. Previous studies aimed at elucidating the early events of arenavirus transcription and genome replication used Northern blot to visualize individual viral RNA species (23, 25, 26). Analysis of RNA from cells infected with LCMV or the New World arenavirus Pichinde failed to detect viral RNA from infected cells prior to 9 hpi (23) or 12 hpi (25), respectively. In the setting of infection with the New World arenavirus Tacaribe, Franze-Fernandez *et al.* detected S genomic RNA and NP mRNA at 2 hpi and S antigenomic RNA at 4 hpi, while GPC mRNA appeared several hours following the synthesis of S antigenomic RNA (26). The earliest the viral L segment has been observed was at 12 hpi (23). In the current study, we are able to detect viral NP and L mRNAs at 1 hpi. Our data supports previous observations that viral NP mRNA expression occurs immediately following infection, and that GPC mRNA expression occurs

Accepted Manuscript Posted Online

Journal of Virology

JVI

Journal of Virology

following a lag of several hours (5, 26). By probing single cells, we build upon this prior work by demonstrating that GPC mRNA expression is not detected, even at low levels, in the first hours following infection. In light of previous observations that antigenomic L and S segment RNAs are packaged in viral particles (20, 26), our inability to observe GPC mRNA in cells immediately following viral entry suggests that S antigenomic RNA packaged in virions is unable to be transcribed. Further, it suggests that GPC mRNAs are not packaged into viral particles, as has been suggested for Z mRNA (43).

An interesting observation from our study was that, despite infecting cells at an MOI of 0.1, ~65-90% of cells expressed one or more genes encoded on the S genomic RNA segment at 6 hpi. Because it takes ~ 8 h for an infected cell to make new infectious progeny (36-39), we were surprised to see such a high frequency of cells expressing these viral mRNAs at a time when the originally-infected cells could not yet have spread virus to additional uninfected cells in the monolayer. Notably, at this same 6 hpi time point, approximately 8% of cells expressed viral L mRNAs, which is consistent with the utilized MOI. One possible explanation for this observation could be that, within the viral stock, there may be a significant population of incomplete viral particles that possess the S segment but lack the L segment genomic RNA or a functional copy of this RNA. Indeed, this phenomenon has been observed for influenza A and Rift Valley Fever virus (44-46). Considering that the genetic basis for how arenavirus DI particles block the propagation of infectious virus particles is unknown, these results may provide clues for future studies to define the mechanism at work. Further examination will be necessary to explain the functional significance of this observation.

A hallmark characteristic of LCMV infection is the ability to establish an asymptomatic, persistent infection in reservoir rodents (47). Further, it is possible to recapitulate key aspects of

Downloaded from http://jvi.asm.org/ on March 6, 2020 at NYU LANGONE MED CTR-SCH OF MED

Accepted Manuscript Posted Online

Journal of Virology

JVI

Journal of Virology

Downloaded from http://jvi.asm.org/ on March 6, 2020 at NYU LANGONE MED CTR-SCH OF MED

this persistent infection in cell culture models of infection (5, 40, 41, 48). One notable characteristic of cell culture models of LCMV infection is the cyclical rise and fall of release of infectious virus seen during persistence (16, 19, 40-42). Several models have been proposed to explain how LCMV restricts its spread to establish and maintain a noncytopathic persistent infection, both *in vitro* and *in vivo*. The first suggests that DI particles, which are produced in abundance by LCMV, can enter permissive host cells and interfere with the ability of standard infectious virus particles to successfully infect and complete the viral life cycle (9-13). Hotchin proposed a second model that he termed cyclical, transient infection. In this model, cells infected with LCMV are initially productive in making infectious virus particles, but later become refractory to superinfection and ultimately clear virus (as evidenced by loss of antigen expression and infectious virus production), only to once again become susceptible to reinfection by the small number of cells that remain productively infected (16-19). Southern and colleagues proposed a third model that was based upon the dynamics and genetic identity of viral RNA species profiled during acute and persistent infection. In particular, they demonstrated by Northern blot that LCMV RNAs (genome, antigenome, and mRNAs) accumulate to high levels during persistence, both *in vitro* and *in vivo* (5, 14, 15, 22). Further, they showed that a proportion of these genomic and antigenomic RNAs, but not mRNAs, contained short deletions in the untranslated regions at their termini (5, 14, 15, 49). They proposed that these deleted RNAs were replication competent, but transcriptionally incompetent. This data suggested a model where, during persistence, viral protein expression and infectious virus production are inhibited due to the accumulation of high levels of transcriptionally defective genomic and antigenomic RNAs. Further, because these deleted RNAs were found in virions, it was proposed that they serve as the molecular basis for DI particle interference. Finally, it was proposed that

Accepted Manuscript Posted Online

Journal of Virology

JVI

Journal of Virology

these deleted RNAs can be repaired by the viral polymerase to initiate bursts of productive replication/infectious virus production during persistence. Each of these models, whether acting independently or in combination, would presumably restrict virus spread, allowing the virus to minimize its impact on host fitness while retaining its ability to propagate and ultimately maintain itself in nature. A potential caveat to the Southern model comes from the finding that the 3' and 5' terminal sequences of the LCMV and LASV genomic RNA species were critical for both the transcription and replication of RNAs in a minigenome reporter assay (50, 51). Thus, the functional significance of these terminally truncated viral RNAs remains to be further elucidated.

The smFISH approach employed in this study can provide insights to build on this prior work. First, our study suggests that cells do not maintain high levels of genomic and antigenomic RNAs throughout persistence. The most likely explanation for the observation of high levels of genome/antigenome during persistence by Southern and colleagues (5, 14, 15, 22) is that they measured viral RNAs from a fraction of the total cells within a population at a particular time point. Second, our findings of large numbers of cells lacking viral RNAs at several persistent time points (which correlates with loss of infectious virus release and antigen expression) suggest that the antigen-negative cells observed by Hotchin et al. (16-19) had either cleared infection or contained undetectable levels of RNA (by smFISH) as opposed to carrying replication-competent, but transcriptionally-incompetent, terminally-deleted genomic/antigenomic RNAs (as the Southern model would suggest (5, 14, 15, 49)). Our smFISH probe sets consisted of pools of 48 short oligo nucleotide probes complementary to different regions spanning entire viral gene sequences. Therefore, even if genomic segments contained short terminal deletions, the majority of smFISH probes would bind their targets, and obvious

Downloaded from http://jvi.asm.org/ on March 6, 2020 at NYU LANGONE MED CTR-SCH OF MED

Accepted Manuscript Posted Online

Journal of Virology

JVI

Journal of Virology

Downloaded from http://jvi.asm.org/ on March 6, 2020 at NYU LANGONE MED CTR-SCH OF MED

smFISH signal would be present by fluorescence microscopy. Our findings also raise several new questions that require further study. For example, it will be important to define the molecular mechanism by which cells clear virus following infection and the specific host machinery responsible. Additionally, it would be particularly interesting to investigate the possibility that cycles of reinfection are jump-started from cells maintaining a reservoir of intracellular infectious virus as has been documented in the literature (52, 53).

In summary, we have used fluorescence microscopy to visualize fluorescently-labeled arenavirus RNA molecules in infected cells. Further, we have described a flexible labeling, imaging, and image analysis pipeline that could be easily adapted to interrogate the events of transcription or genomic replication of any RNA virus, particularly where it is critical to image and quantify RNA levels in hundreds to thousands of cells per experimental condition. We have taken advantage of this pipeline to examine the transcription and replication kinetics of LCMV RNAs over the course of infection. In particular, our data support the transient, cyclical infection model originally proposed by Hotchin (16-19) and suggest that, following a period of productive infection, cells can clear infection, including viral genetic material and antigen, before becoming susceptible to reinfection. Further, our data provides some support for the ideas that viral antigenomic RNA in virions may not be transcriptionally functional upon virus entry and that a significant fraction of virus particles may lack functional L genomic RNA, an observation that remains to be fully explored. Developing the ability to label genomic and antigenomic RNAs with greater sensitivity will be an important next step toward the construction of a quantitative model of the regulation of viral RNA replication and transcription over time with the goal of explaining the oscillatory behavior of viral RNA synthesis during persistence. While the cell culture model of persistent infection has provided interesting observations, it will be particularly

Accepted Manuscript Posted Online

Journal of Virology

JVI

Journal of Virology

Downloaded from http://jvi.asm.org/ on March 6, 2020 at NYU LANGONE MED CTR-SCH OF MED

important to examine how the genetic events of transcription and replication are regulated in an *in vivo* model of persistent infection in future studies.

MATERIALS AND METHODS

Cells and Viruses. A549 (CCL-185) were obtained from American Type Culture Collection (ATCC, Manassas, VA). A549 cells were cultured in DMEM-F12 (11320-033, Thermo Fisher), containing 10% fetal bovine serum and 1% Penicillin-Streptomycin (15140-163, Thermo Fisher). LCMV Armstrong 53b was provided by J. L. Whitton (The Scripps Research institute, La Jolla, CA). A549 cells were infected with LCMV Arm53b at an MOI of 0.1 (Fig. 5 to 6) or an MOI of 0.01 (Fig. 1, 2, 4, 7, 8, 9, and 10). For experiments examining late, persistent time points following infections, a T25 tissue culture flask of A549 cells was infected. The flask of infected cells was trypsinized and cells were plated on glass coverslips 24 hours prior to the reported time points where cover slips were fixed, stained, and imaged as described below (Fig. 10). Remaining cells were diluted and re-plated in a T25 flask until 24 hours before the next examined time point where this process was repeated. Standard plaque assay on Vero E6 cells was used to determine the titer of infectious LCMV in collected supernatants. No cytopathic effect was observed in persistently infected cultures.

Single molecule RNA-FISH. Cells were plated on 14 mm round #1 glass coverslips. Following infection, cells were briefly washed in room temperature DPBS (with Calcium and Magnesium) (14040133, Thermo Fisher) and fixed in 4% PFA in 1x PBS for 10 minutes at room temperature. Coverslips were washed twice in room temperature PBS and fixed again at -20° C with 70% ethanol for at least two hours. Coverslips were washed twice with 2x SSC (AM9770,

Accepted Manuscript Posted Online

Journal of Virology

JVI

Journal of Virology

Downloaded from http://jvi.asm.org/ on March 6, 2020 at NYU LANGONE MED CTR-SCH OF MED

457 Thermo Fisher) and washed once with 2x SSC and 10% Formamide (BP227, Fisher Scientific).
458 smFISH probes to different viral RNA species (Fig. 1A) were designed using the Stellaris Probe
459 Designer at https://www.biosearchtech.com/ (Table S1). Unlabeled smFISH probes had a 3'
460 modified base with an amine functional group. Pools of 48 individual smFISH probes to a
461 particular target RNA were combined at equimolar ratios and were covalently labeled with Cy3
462 (PA23001, GE Healthcare), AlexaFluor 568 (A20003, Thermo Fisher), or Cy5 (PA25001, GE
463 Healthcare) as previously described (54). Coverslips were placed face down on a 100 ul drop of
464 hybridization mix containing 75 ng of smFISH probe dissolved in hybridization buffer composed
465 of 10% dextran sulfate (D8906, Sigma-Aldrich), 2x SSC, and 10% Formamide. Hybridization
466 occurred in a humidified chamber at 37° C overnight. Coverslips were washed twice in 2x SSC,
467 10% formamide at 37° C for 30 minutes. Coverslips were then washed once in 1x PBS. For
468 cellular segmentation, cells were stained with HCS CellMask™ Green stain (H32714, Thermo
469 Fisher) diluted at 50 ng/ml in PBS for 5 minutes at room temperature (note: this is significantly
470 more dilute than recommended in the product information, but we found it necessary to prevent
471 overstaining cells and thus to prevent spectral bleed through into the AlexaFluor 568
472 fluorescence channel). Nuclei were stained with 4', 6-diamidino-2-phenylindole hydrochloride
473 30 (DAPI) (D9542, Sigma-Aldrich) at 1 µg/ml in PBS for 5 minutes at room temperature. Cells
474 were washed a final time in PBS, briefly washed in water, dried and mounted with ProLong Gold
475 Antifade Reagent (P36934, Thermo Fisher).

476 Combined immunofluorescence and smFISH staining protocols were performed as
477 previously described (55). LCMV nucleoprotein (NP) was labeled with antibody 1-1.3 and
478 glyocoprotein (GPC) was labeled with antibody 33.6 (both from M. Buchmeier, University of

Accepted Manuscript Posted Online

Journal of Virology

JVI

Journal of Virology

Downloaded from http://jvi.asm.org/ on March 6, 2020 at NYU LANGONE MED CTR-SCH OF MED

California Irvine). Primary antibodies were visualized with a secondary Alexa Fluor 488-conjugated goat anti-mouse IgG (H+L) (A-11029, Thermo Scientific).

Image Acquisition. Wide-field fluorescent Z-stacks were acquired using a Nikon Ti Eclipse microscope with a 60 × 1.4 NA objective. Samples were illuminated with an LED light-source (Lumencor Spectra X light engine) with appropriate filter sets and images were captured with a Hamamatsu Orca flash 4.0 LT sCMOS camera. Z-stacks were captured at 300 nm increments, and the microscope was controlled by Nikon NIS Elements software. Captured ND2 images were converted to Tiffs using the open source Bio-formats tool kit (http://www.openmicroscopy.org/) (56).

Image Segmentation and Analysis. DAPI and CellMask Green Z-stacks were projected using a focus-based projection method as previously described (57). Projected DAPI images were used for automatic nuclear segmentation in CellProfiler (Broad Institute) (34) and served as the seed for automatic secondary cellular segmentation using the projected CellMask Green images (Fig. 4A). Statistics including average pixel intensity within the regions defined by primary and secondary segmentation were extracted from maximum intensity projections of smFISH Z-stacks using CellProfiler (Fig. 4B to D).

Single smFISH labeled RNAs were detected and localized in 3D using FISH-quant (35). Briefly, smFISH Z-stacks were filtered using the “Dual Gaussian Filter” and spots were detected using the “Local Maximum” method. As a large number of acquired images required analysis, images were analyzed in “Batch Mode” with settings determined to give low rates of false positive detections. The signal-to-noise ratio of different smFISH probe sets was determined as the average signal amplitude of identified smFISH spots in an individual cell divided by the

Accepted Manuscript Posted Online

Journal of Virology

JVI

Journal of Virology

standard deviation of the fluorescent signal in a region of the same cell where smFISH spots were absent (Fig 3).

Box and whisker plots were created using the ggplot2 package in R. The box represents the interquartile range of the data with the center line representing the median. Individual dots represent cells that are more than 1.5 times the interquartile range away from the median of the data.

FUNDING INFORMATION

We also gratefully acknowledge funding support from NIH grants T32 HL076122-10 (BRK), T32 AI055402 (CMZ), R21 AI088059 (JB), and P20RR021905 & P30GM118228 (Immunobiology and Infectious Disease COBRE awards) (JB). DZ is supported by the Canadian Institute for Health Research (Project Grant-366682), Fond de recherche du Quebec (Chercheur-boursier Junior 2), and the Canadian Foundation for Innovation. CZ, FM, and AS were supported by Institut Pasteur and the Fondation pour la Recherche Médicale (FRM). BRK was supported by a Chateaubriand fellowship from the Office for Science & Technology at the Embassy of France in the United States. The funders had no role in study design, data collection and analysis, decision to publish, or preparation of the manuscript.

ACKNOWLEDGEMENTS

We gratefully acknowledge J. Lindsay Whitton for providing us with LCMV strain Arm53b and Samir Rahman, Philippe Clerc, Christian Weber, and Sophie Abélanet for technical assistance.

Downloaded from http://jvi.asm.org/ on March 6, 2020 at NYU LANGONE MED CTR-SCH OF MED

Accepted Manuscript Posted Online

We thank Pablo Navarro and Jason Stumpff for graciously offering the use of their microscopy equipment and for providing their expertise and Jean-Michel Arbona and Wei Ouyang for helpful discussions.

REFERENCES

1. Buchmeier MJ, de la Torre JC, Peters CJ. 2007. Arenaviridae: The Viruses and Their Replication, p 1791-1827. *In* Knipe DM, Howley PM, Griffin DE, Lamb RA, Martin MA, Roizman B, Straus SE (ed), Fields Virology. Wolters Kluwer Heath/Lippincott Williams & Wilkins, Philadelphia.
2. Fischer SA, Graham MB, Kuehnert MJ, Kotton CN, Srinivasan A, Marty FM, Comer JA, Guarner J, Paddock CD, DeMeo DL, Shieh WJ, Erickson BR, Bandy U, DeMaria A, Jr., Davis JP, Delmonico FL, Pavlin B, Likos A, Vincent MJ, Sealy TK, Goldsmith CS, Jernigan DB, Rollin PE, Packard MM, Patel M, Rowland C, Helfand RF, Nichol ST, Fishman JA, Ksiazek T, Zaki SR, Team LiTRI. 2006. Transmission of lymphocytic choriomeningitis virus by organ transplantation. N Engl J Med 354:2235-49.
3. Enria DA, Briggiler AM, Sanchez Z. 2008. Treatment of Argentine hemorrhagic fever. Antiviral Res 78:132-9.
4. McCormick JB, King IJ, Webb PA, Scribner CL, Craven RB, Johnson KM, Elliott LH, Belmont-Williams R. 1986. Lassa fever. Effective therapy with ribavirin. N Engl J Med 314:20-6.
5. Meyer BJ, de la Torre JC, Southern PJ. 2002. Arenaviruses: genomic RNAs, transcription, and replication. Curr Top Microbiol Immunol 262:139-57.

Journal of Virology
JVI
Journal of Virology
Downloaded from http://jvi.asm.org/ on March 6, 2020 at NYU LANGONE MED CTR-SCH OF MED

Accepted Manuscript Posted Online

6. Buchmeier MJ, Zajac AJ. 1999. Lymphocytic choriomeningitis virus, p x, 725 p. *In* Ahmed R, Chen I (ed), Persistent viral infections. John Wiley & Sons, Chichester ; New York.

7. Buchmeier MJ, Welsh RM, Dutko FJ, Oldstone MB. 1980. The virology and immunobiology of lymphocytic choriomeningitis virus infection. Adv Immunol 30:275-331.

8. Lehmann-Grube F, Martinez Peralta LM, Bruns M, Lohler J. 1983. Persistent infection of mice with the lymphocytic choriomeningitis virus, p 43-103. *In* Fraenkel-Conrat H, Wagner RR (ed), Virus-host interactions, receptors, persistence, and neurological diseases. Plenum Press, New York.

9. Burns JW, Buchmeier MJ. 1993. Glycoproteins of the arenaviruses, p 17-35. *In* Salvato MS (ed), The Arenaviridae. Plenum Press, New York.

10. Huang AS, Baltimore D. 1970. Defective viral particles and viral disease processes. Nature 226:325-7.

11. Oldstone MB. 1998. Viral persistence: mechanisms and consequences. Curr Opin Microbiol 1:436-41.

12. Huang AS. 1973. Defective interfering viruses. Annu Rev Microbiol 27:101-17.

13. Welsh RM, O'Connell CM, Pfau CJ. 1972. Properties of defective lymphocytic choriomeningitis virus. J Gen Virol 17:355-9.

14. Meyer BJ, Southern PJ. 1994. Sequence heterogeneity in the termini of lymphocytic choriomeningitis virus genomic and antigenomic RNAs. J Virol 68:7659-64.

Journal of Virology

JVI

Journal of Virology

Downloaded from http://jvi.asm.org/ on March 6, 2020 at NYU LANGONE MED CTR-SCH OF MED

Accepted Manuscript Posted Online

15. Meyer BJ, Southern PJ. 1997. A novel type of defective viral genome suggests a unique strategy to establish and maintain persistent lymphocytic choriomeningitis virus infections. J Virol 71:6757-64.

16. Hotchin J. 1974. Cyclical phenomena in persistent virus infection. J Reticuloendothel Soc 15:304-11.

17. Hotchin J. 1974. The role of transient infection in arenavirus persistence. Prog Med Virol 18:81-93.

18. Hotchin J. 1973. Transient virus infection: spontaneous recovery mechanism of lymphocytic choriomeningitis virrus-infected cells. Nat New Biol 241:270-2.

19. Hotchin J, Kinch W, Benson L, Sikora E. 1975. Role of substrains in persistent lymphocytic choriomeningitis virus infection. Bull World Health Organ 52:457-63.

20. Haist K, Ziegler C, Botten J. 2015. Strand-Specific Quantitative Reverse Transcription-Polymerase Chain Reaction Assay for Measurement of Arenavirus Genomic and Antigenomic RNAs. PLoS One 10:e0120043.

21. Francis SJ, Southern PJ. 1988. Deleted viral RNAs and lymphocytic choriomeningitis virus persistence in vitro. J Gen Virol 69 (Pt 8):1893-902.

22. Francis SJ, Southern PJ. 1988. Molecular analysis of viral RNAs in mice persistently infected with lymphocytic choriomeningitis virus. J Virol 62:1251-7.

23. Fuller-Pace FV, Southern PJ. 1988. Temporal analysis of transcription and replication during acute infection with lymphocytic choriomeningitis virus. Virology 162:260-3.

24. Southern PJ, Singh MK, Riviere Y, Jacoby DR, Buchmeier MJ, Oldstone MB. 1987. Molecular characterization of the genomic S RNA segment from lymphocytic choriomeningitis virus. Virology 157:145-55.

Downloaded from http://jvi.asm.org/ on March 6, 2020 at NYU LANGONE MED CTR-SCH OF MED

Journal of Virology JVI Journal of Virology

Accepted Manuscript Posted Online

588 25. Shivaprakash M, Harnish D, Rawls W. 1988. Characterization of temperature-sensitive
589 mutants of Pichinde virus. J Virol 62:4037-43.
590 26. Franze-Fernandez MT, Zetina C, Iapalucci S, Lucero MA, Bouissou C, Lopez R, Rey O,
591 Daheli M, Cohen GN, Zakin MM. 1987. Molecular structure and early events in the
592 replication of Tacaribe arenavirus S RNA. Virus Res 7:309-24.
593 27. Auperin DD, Romanowski V, Galinski M, Bishop DH. 1984. Sequencing studies of
594 pichinde arenavirus S RNA indicate a novel coding strategy, an ambisense viral S RNA. J
595 Virol 52:897-904.
596 28. Polyak SJ, Zheng S, Harnish DG. 1995. Analysis of Pichinde arenavirus transcription and
597 replication in human THP-1 monocytic cells. Virus Res 36:37-48.
598 29. Fuller-Pace FV, Southern PJ. 1989. Detection of virus-specific RNA-dependent RNA
599 polymerase activity in extracts from cells infected with lymphocytic choriomeningitis
600 virus: in vitro synthesis of full-length viral RNA species. J Virol 63:1938-44.
601 30. Raj A, van den Bogaard P, Rifkin SA, van Oudenaarden A, Tyagi S. 2008. Imaging
602 individual mRNA molecules using multiple singly labeled probes. Nat Methods 5:877-9.
603 31. Zenklusen D, Larson DR, Singer RH. 2008. Single-RNA counting reveals alternative
604 modes of gene expression in yeast. Nat Struct Mol Biol 15:1263-71.
605 32. King BR, Kellner S, Eisenhauer PL, Bruce EA, Ziegler CM, Zenklusen D, Botten JW.
606 2017. Visualization of the lymphocytic choriomeningitis mammarenavirus (LCMV)
607 genome reveals the early endosome as a possible site for genome replication and viral
608 particle pre-assembly. J Gen Virol doi:10.1099/jgv.0.000930.
609 33. Ziegler CM, Eisenhauer P, Bruce EA, Weir ME, King BR, Klaus JP, Krementsov DN,
610 Shirley DJ, Ballif BA, Botten J. 2016. The Lymphocytic Choriomeningitis Virus Matrix

Downloaded from http://jvi.asm.org/ on March 6, 2020 at NYU LANGONE MED CTR-SCH OF MED

Journal of Virology JVI Journal of Virology

Accepted Manuscript Posted Online

Protein PPXY Late Domain Drives the Production of Defective Interfering Particles. PLoS Pathog 12:e1005501.

34. Kamentsky L, Jones TR, Fraser A, Bray MA, Logan DJ, Madden KL, Ljosa V, Rueden C, Eliceiri KW, Carpenter AE. 2011. Improved structure, function and compatibility for CellProfiler: modular high-throughput image analysis software. Bioinformatics 27:1179-80.

35. Mueller F, Senecal A, Tantale K, Marie-Nelly H, Ly N, Collin O, Basyuk E, Bertrand E, Darzacq X, Zimmer C. 2013. FISH-quant: automatic counting of transcripts in 3D FISH images. Nat Methods 10:277-8.

36. Buchmeier MJ, Elder JH, Oldstone MB. 1978. Protein structure of lymphocytic choriomeningitis virus: identification of the virus structural and cell associated polypeptides. Virology 89:133-45.

37. Dutko FJ, Pfau CJ. 1978. Arenavirus defective interfering particles mask the cell-killing potential of standard virus. J Gen Virol 38:195-208.

38. Lehmann-Grube F, Popescu M, Schaefer H, Gschwender HH. 1975. LCM virus infection of cells in vitro. Bull World Health Organ 52:443-56.

39. Lehmann-Grube F. 1971. Lymphocytic choriomeningitis virus, vol 10. Springer-Verlag, Wien.

40. Lehmann-Grube F. 1967. A carrier state of lymphocytic choriomeningitis virus in L cell cultures. Nature 213:770-3.

41. Lehmann-Grube F, Slenczka W, Tees R. 1969. A persistent and inapparent infection of L cells with the virus of lymphocytic choriomeningitis. J Gen Virol 5:63-81.

Journal of Virology

JVI

Journal of Virology

Downloaded from http://jvi.asm.org/ on March 6, 2020 at NYU LANGONE MED CTR-SCH OF MED

Accepted Manuscript Posted Online

633 42. Staneck LD, Trowbridge RS, Welsh RM, Wright EA, Pfau CJ. 1972. Arenaviruses:
634 cellular response to long-term in vitro infection with parana and lymphocytic
635 choriomeningitis viruses. Infect Immun 6:444-50.
636 43. Salvato MS, Shimomaye EM. 1989. The completed sequence of lymphocytic
637 choriomeningitis virus reveals a unique RNA structure and a gene for a zinc finger
638 protein. Virology 173:1-10.
639 44. Fonville JM, Marshall N, Tao H, Steel J, Lowen AC. 2015. Influenza Virus Reassortment
640 Is Enhanced by Semi-infectious Particles but Can Be Suppressed by Defective Interfering
641 Particles. PLoS Pathog 11:e1005204.
642 45. Wichgers Schreur PJ, Kortekaas J. 2016. Single-Molecule FISH Reveals Non-selective
643 Packaging of Rift Valley Fever Virus Genome Segments. PLoS Pathog 12:e1005800.
644 46. Brooke CB, Ince WL, Wrammert J, Ahmed R, Wilson PC, Bennink JR, Yewdell JW.
645 2013. Most influenza a virions fail to express at least one essential viral protein. J Virol
646 87:3155-62.
647 47. Francis SJ, Southern PJ, Valsamakis A, Oldstone MB. 1987. State of viral genome and
648 proteins during persistent lymphocytic choriomeningitis virus infection. Curr Top
649 Microbiol Immunol 133:67-88.
650 48. Oldstone MB, Buchmeier MJ. 1982. Restricted expression of viral glycoprotein in cells
651 of persistently infected mice. Nature 300:360-2.
652 49. Meyer BJ, Southern PJ. 1993. Concurrent sequence analysis of 5' and 3' RNA termini by
653 intramolecular circularization reveals 5' nontemplated bases and 3' terminal heterogeneity
654 for lymphocytic choriomeningitis virus mRNAs. J Virol 67:2621-7.

Downloaded from http://jvi.asm.org/ on March 6, 2020 at NYU LANGONE MED CTR-SCH OF MED

Journal of Virology

JVI

Journal of Virology

Accepted Manuscript Posted Online

50. Perez M, de la Torre JC. 2003. Characterization of the genomic promoter of the prototypic arenavirus lymphocytic choriomeningitis virus. J Virol 77:1184-94.

51. Hass M, Westerkofsky M, Muller S, Becker-Ziaja B, Busch C, Gunther S. 2006. Mutational analysis of the lassa virus promoter. J Virol 80:12414-9.

52. van der Zeijst BA, Noyes BE, Mirault ME, Parker B, Osterhaus AD, Swyryd EA, Bleumink N, Horzinek MC, Stark GR. 1983. Persistent infection of some standard cell lines by lymphocytic choriomeningitis virus: transmission of infection by an intracellular agent. J Virol 48:249-61.

53. Stanwick TL, Kirk BE. 1976. Analysis of baby hamster kidney cells persistently infected with lymphocytic choriomeningitis virus. J Gen Virol 32:361-7.

54. Zenklusen D, Singer RH. 2010. Analyzing mRNA expression using single mRNA resolution fluorescent in situ hybridization. Methods Enzymol 470:641-59.

55. Song T, Zheng Y, Wang Y, Katz Z, Liu X, Chen S, Singer RH, Gu W. 2015. Specific interaction of KIF11 with ZBP1 regulates the transport of beta-actin mRNA and cell motility. J Cell Sci 128:1001-10.

56. Goldberg IG, Allan C, Burel JM, Creager D, Falconi A, Hochheiser H, Johnston J, Mellen J, Sorger PK, Swedlow JR. 2005. The Open Microscopy Environment (OME) Data Model and XML file: open tools for informatics and quantitative analysis in biological imaging. Genome Biol 6:R47.

57. Tsanov N, Samacoits A, Chouaib R, Traboulsi AM, Gostan T, Weber C, Zimmer C, Zibara K, Walter T, Peter M, Bertrand E, Mueller F. 2016. smiFISH and FISH-quant - a flexible single RNA detection approach with super-resolution capability. Nucleic Acids Res 44:e165.

Journal of Virology

JVI

Journal of Virology

Downloaded from http://jvi.asm.org/ on March 6, 2020 at NYU LANGONE MED CTR-SCH OF MED

Accepted Manuscript Posted Online

Journal of Virology

JVI

Journal of Virology

Downloaded from http://jvi.asm.org/ on March 6, 2020 at NYU LANGONE MED CTR-SCH OF MED

678

679 **FIGURE LEGENDS**

680 FIG 1 LCMV RNA species can be specifically visualized using multiple, singly-labeled
681 oligonucleotide smFISH probes.

682 (A) Overview of the scheme used by arenaviruses to transcribe and replicate their single-
683 stranded, ambisense, bisegmented genome. smFISH probes that recognize the S segment
684 genomic RNA are shown in gray, probes that recognize the S segment genome and GPC mRNA
685 are shown in red, probes that recognize the S segment antigenome and NP mRNA are shown in
686 green, and probes that recognize the L segment antigenome and L mRNA are shown in pink.
687 smFISH probe sets consist of pools of 48 individual 20mer oligonucleotides each labeled with a
688 single fluorophore at their 3' terminus. (B) Uninfected cells were stained with a control smFISH
689 probe set specific to the cellular mRNA MDN1 labeled with Cy3. (C) Cells were either infected
690 with LCMV at an MOI of 0.01 or, as a control, remained uninfected (mock). Cells were fixed at
691 24 hpi and stained with a Cy5-labeled smFISH probe set specific for S segment genomic RNA
692 and GPC mRNA. Boxed regions of the cell are magnified and shown in columns labeled
693 "Zoom". Green arrows indicate example smFISH stained spots most likely representing single
694 labeled RNAs. Nuclear (hatched line) and cytoplasmic (solid line) boundaries are shown in blue.
695 The same intensity levels for a particular probe set were applied to all images of mock- and
696 LCMV-infected cells to permit comparisons. Scale bars are 10 μm.

697

698 FIG 2 smFISH probe sets recognizing viral mRNA species exhibit high signal-to-noise staining.

Accepted Manuscript Posted Online

Journal of Virology

JVI

Journal of Virology

Downloaded from http://jvi.asm.org/ on March 6, 2020 at NYU LANGONE MED CTR-SCH OF MED

699 Mock- or LCMV-infected cells (24 hr pi) were simultaneously stained with smFISH probe sets
700 specific for either GPC mRNA and S genome (Cy5; green) or S genome only (AlexaFluor 568;
701 red). Representative LCMV infected cells with moderate (A) or high (B) levels of viral RNA as
702 well as a representative mock-infected cell (C) are displayed. Multiple Z stacks were acquired
703 spanning the thickness of the cell and max intensity projections are displayed. Boxed regions of
704 the cell are magnified and shown in rows labeled "Zoom". Nuclear (hatched line) and
705 cytoplasmic (solid line) boundaries are shown in blue. (A to C) The same intensity levels for a
706 particular probe set were applied to all images of mock- and LCMV-infected cells to permit
707 comparisons. Scale bars are 10 μm.

708

709 FIG 3. smFISH probe sets recognizing viral mRNA species exhibit high signal-to-noise staining

710 Signal-to-noise ratio of different smFISH probe sets labeled with the indicated fluorophores.
711 Signal-to-noise ratio was calculated as average amplitude of detected smFISH spots divided by
712 the standard deviation of signal in a region of the cell with no detected spots. The signal-to-noise
713 ratio of 20 cells per smFISH probe set labeled with the indicated fluorophore was calculated, and
714 the mean and standard deviation are graphed.

715

716 FIG 4 Automated detection and quantitation of LCMV RNAs labeled with spectrally distinct
717 fluorophores.

718 (A) Cell nuclei and cytoplasms were automatically segmented using focus-based projections of
719 DAPI (nuclei) or CellMask Green (cytoplasm) Z stacks acquired through the thickness of the
720 cell. Note that pixel intensities of the CellMask Green projection displayed here have been log

Accepted Manuscript Posted Online

Journal of Virology

JVI

Journal of Virology

Downloaded from http://jvi.asm.org/ on March 6, 2020 at NYU LANGONE MED CTR-SCH OF MED

721 transformed to aid visualization. Nuclear (hatched line) and cytoplasmic (solid line) boundaries
722 are shown in white. The scale bar is 10 μm.

723 (B and C) Maximum intensity projections of LCMV-infected cells were fixed 24 hpi and stained
724 with smFISH probe sets to the NP mRNA/S antigenome (Cy5; green) and GPC mRNA/S
725 genome (A568; red). The boxed region of each cell is magnified and shown in the row labeled
726 "Zoom". Cells were segmented based on DAPI and CellMask Green staining (see panel A) and
727 spots were detected and localized in 3D using FISH-quant. Individually detected RNAs are
728 circled in green (NP mRNA/S antigenome) or red (GPC mRNA/S genome). The "Spots only"
729 column shows only the position of detected spots in relation to the cell boundaries defined by
730 segmentation. Nuclear (hatched line) and cytoplasmic (solid line) boundaries are shown in blue.
731 The same intensity levels for a particular probe set were applied to both images of LCMV-
732 infected cells to permit comparisons. The scale bar is 10 μm.

733 (D) Scatter plot shows the relationship between the fluorescence intensity in the smFISH channel
734 in the maximum intensity projection of smFISH images and the number of smFISH spots
735 detected by FISH-quant for LCMV-infected cells fixed 24 hpi and stained with the Cy5-labeled
736 smFISH probes specific for NP mRNA/S antigenome.

737

738 FIG 5 Transcription of NP and L genes is detectable soon following infection while GPC
739 transcription exclusively occurs after a several hour lag.

740 Cells were infected with LCMV at an MOI of 0.1, fixed at various times following infection, and
741 stained for NP mRNA (green) using a Cy5-labeled NP mRNA/S antigenome probe set, GPC
742 mRNA (red) using an A568-labled GPC mRNA/S genome probe set (A) or NP mRNA (green)

Accepted Manuscript Posted Online

using an A568-labeled NP mRNA/S antigenome probe set and L mRNA (magenta) using a Quasar 670-labeled L mRNA/L antigenome probe set (B). Note that for the time points shown (less than 8 hpi), genomic and antigenomic RNAs are not detectable by smFISH probe sets with exclusive specificity for these RNAs (data not shown). Therefore, spots detected in this figure are presumed to represent only the mRNAs, but not the genome or antigenome, targeted by each respective probe set. Nuclear (hatched line) and cytoplasmic (solid line) boundaries as determined by Cell Profiler are shown in blue. Identified spots are outline by circles that are green for NP mRNA, red for GPC mRNA, and magenta for L mRNA. (A and B) The same intensity levels for a particular probe set were applied to all images of mock- and LCMV-infected cells across the time course to permit comparisons. Representative maximum intensity projections from 1 of 2 independent experiments are shown. Scale bar is 10 μm.

FIG 6 Transcription of NP and L genes is detectable immediately upon infection while GPC transcription exclusively occurs after a several hour lag.

Related to Fig. 5. (A and B) Boxplots represent the number of viral RNAs detected in cells at early time points following infection with LCMV (see Figure 5). (C and D) Stacked bar graphs show the proportion of cells expressing RNAs detected by one, both, or neither viral RNA smFISH probe set. Between 620 and 1316 cells were examined at each time point. In each case RNAs identified by specific probe sets are designated by color (green for NP mRNA/S antigenome probes, red for GPC mRNA/S genome probes, and magenta for L mRNA/L antigenome probes). Note that for time points prior to 8 hpi, genomic and antigenomic RNAs are not detectable by smFISH probe sets with exclusive specificity for these RNAs (data not shown). Therefore, spots detected before 8 hpi are presumed to represent only the mRNAs, but not the

Downloaded from http://jvi.asm.org/ on March 6, 2020 at NYU LANGONE MED CTR-SCH OF MED

Journal of Virology JVI Journal of Virology

Accepted Manuscript Posted Online

Journal of Virology

JVI

Journal of Virology

Downloaded from http://jvi.asm.org/ on March 6, 2020 at NYU LANGONE MED CTR-SCH OF MED

766 genome or antigenome, recognized by each respective probe set. Spots detected at 8 hpi or later
767 are presumed to be a mixture of all RNAs recognized by a particular probe set (e.g. mRNA and
768 genome or antigenome).

769

770 FIG 7 Peak viral RNA replication and transcription occurs 36 hpi and is slowly lost from
771 infected cells over the following days.

772 Cells were infected with LCMV at an MOI of 0.01, fixed at various times following infection,
773 and stained using smFISH probe sets specific for NP mRNA/S antigenome (Cy5; green) and
774 GPC mRNA/S genome (A568; red) (A) or NP mRNA/S antigenome (A568; green) and L
775 mRNA/L antigenome (Quasar 670; magenta) (B). (A and B) Representative maximum intensity
776 projections of fields of infected cells at various time points from 1 of 2 independent experiments
777 are shown. Each probe set is shown in its own row to highlight the difference in levels to which
778 these RNAs accumulate. The same intensity levels for a particular probe set were applied to all
779 images of mock- and LCMV-infected cells across the time course to permit comparisons. Scale
780 bars = 10 μm.

781

782 FIG 8 Peak viral RNA replication and transcription occurs 36 hpi and is slowly lost from
783 infected cells over the following days.

784 Related to Fig. 7. (A and B) Boxplots represent the number of mRNAs detected in cells at time
785 points during the peak period of LCMV infection. (C and D) Stacked bar graph shows the
786 proportion of cells expressing RNAs detected by one, both, or neither viral smFISH probe set.
787 Between 480 and 1659 cells were examined at each time point. RNAs identified by specific

Accepted Manuscript Posted Online

Journal of Virology

JVI

Journal of Virology

Downloaded from http://jvi.asm.org/ on March 6, 2020 at NYU LANGONE MED CTR-SCH OF MED

788 probe sets are designated by color (green for NP mRNA/S antigenome probes, red for GPC
789 mRNA/S genome probes, and magenta for L mRNA/L antigenome probes).

790

791 FIG 9 Cyclic periods of infectious virus particle release and antigen expression during
792 persistence.

793 Cells were infected with LCMV at an MOI of 0.01. (A) Supernatants from infected cells were
794 collected at indicated time points post infection, titered, and the data are presented as mean
795 PFU/ml ± SD from 3 independent experiments. (B to C) Cells were fixed at the indicated time
796 points following infection and stained using smFISH probe sets specific for NP mRNA/S
797 antigenome (A568; red), GPC mRNA/S genome (Cy5; magenta), and NP protein (Alexa 488;
798 green) (B) or GPC protein (Alexa 488; green) (C). A single Z slice of a representative field of
799 infected cells at various time points is shown. Each antibody or probe set is shown in its own row
800 and the same intensity levels were applied to all images of mock- and LCMV-infected cells
801 across the time course to permit comparisons. Scale bar is 10 μm.

802

803 FIG 10 Cyclic periods of viral RNA production and viral RNA loss occur during persistence.

804 Cells were infected with LCMV at an MOI of 0.01, fixed at the indicated time points following
805 infection, and stained using smFISH probe sets specific for NP mRNA/S antigenome (Cy5;
806 green) and GPC mRNA/S genome (A568; red) (A) or NP mRNA/S antigenome (A568; green)
807 and L mRNA/L antigenome (Quasar 670; magenta) (D). (A and D) Representative maximum
808 intensity projections of fields of infected cells at various time points from 1 of 2 independent
809 experiments are shown. Each probe set is shown in its own row to highlight the difference in

Accepted Manuscript Posted Online

Journal of Virology

JVI

Journal of Virology

levels to which these RNAs accumulate. The same intensity levels for a particular probe set were applied to all images of mock- and LCMV-infected cells across the time course to permit comparisons. Scale bar is 10 µm. (B and E) Line graphs show the average number of the indicated viral RNAs detected in cells at time points during the persistent phase of LCMV infection. (C and F) Stacked bar graph shows the proportion of cells expressing RNAs detected by one, both, or neither viral smFISH probe set. Between 316 and 1218 cells were examined at each time point.

Downloaded from http://jvi.asm.org/ on March 6, 2020 at NYU LANGONE MED CTR-SCH OF MED

Accepted Manuscript Posted Online

Journal of Virology

JVI

Journal of Virology

Downloaded from http://jvi.asm.org/ on March 6, 2020 at NYU LANGONE MED CTR-SCH OF MED

817 **Table 1: Ratio in the expression levels of viral mRNAs in individual infected cells.**

	Time points	*Ratio NP mRNA and S antigenome /GPC mRNA and S genome (± SD)*	*Ratio NP mRNA and S antigenome /L mRNA and L antigenome (± SD)*
Early time points (hpi) MOI = 0.1	0.5	ND	ND
	1	ND	ND
	2	ND	ND
	3	ND	ND
	4[a]	4.3 ± 3.4	ND
	6[a]	6.0 ± 4.0	14.7 ± 9.5
	8	4.9 ± 4.1	14.8 ± 12.1
	10	5.6 ± 5.4	12.5 ± 9.7
	12	5.0 ± 4.9	10.8 ± 9.5
Peak time points (hpi) MOI = 0.01	12	4.6 ± 4.1	8.8 ± 6.7
	24	3.5 ± 3.4	14.8 ± 7.2
	36	2.3 ± 1.9	18.0 ± 12.8
	48	2.2 ± 1.2	28.7 ± 14.8
	60	2.9 ± 1.2	34.1 ± 13.3
	72	2.9 ± 1.1	30.1 ± 16.2
	96	4.0 ± 1.9	24.5 ± 13.4
Persistent time (dpi) MOI = 0.01	1.5	2.3 ± 1.6	10.2 ± 12.3
	4	4.3 ± 2.0	10.5 ± 10.4
	6	3.9 ± 2.4	4.9 ± 6.8
	8	1.0 ± 0.7	2.0 ± 3.0
	13	4.4 ± 2.8	24.1 ± 23.9
	16	1.8 ± 1.7	2.4 ± 3.5
	20	6.2 ± 3.7	28.1 ± 23.5
	23	3.2 ± 2.0	5.8 ± 7.3
	27	4.9 ± 4.2	2.7 ± 4.5
	30	4.0 ± 2.3	9.1 ± 8.9
	34	0.7 ± 1.2	2.2 ± 3.4
	37	4.5 ± 3.8	6.1 ± 9.1
	41	1.0 ± 1.3	7.3 ± 9.0

818 [a]Note that for time points prior to 8 hpi, genomic and antigenomic RNAs are not detectable by
819 smFISH probe sets with exclusive specificity for these RNAs (data not shown). Therefore, spots
820 detected before 8 hpi are presumed to represent only the mRNAs, but not the genome or
821 antigenome, recognized by each respective probe set. Spots detect at 8 hpi or later are presumed

Accepted Manuscript Posted Online

Journal of Virology

JVI

Journal of Virology

822 to be a mixture of all RNAs recognized by a particular probe set (e.g. mRNA and genome or
823 antigenome).

824

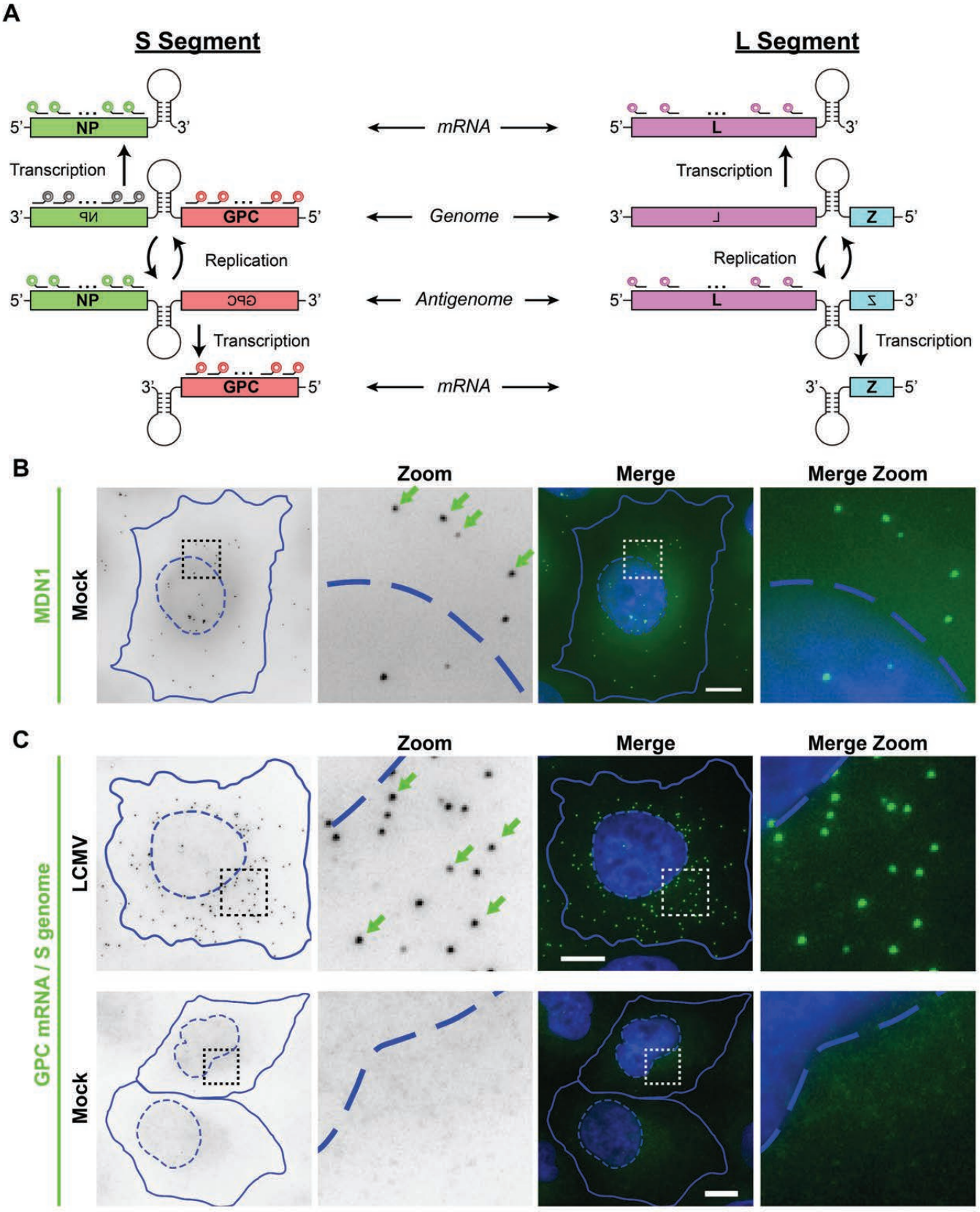
Downloaded from http://jvi.asm.org/ on March 6, 2020 at NYU LANGONE MED CTR-SCH OF MED

Accepted Manuscript Posted Online

Journal of Virology

JVI

Journal of Virology



Downloaded from http://jvi.asm.org/ on March 6, 2020 at NYU LANGONE MED CTR-SCH OF MED

Accepted Manuscript Posted Online

Journal of Virology

JVI

Journal of Virology

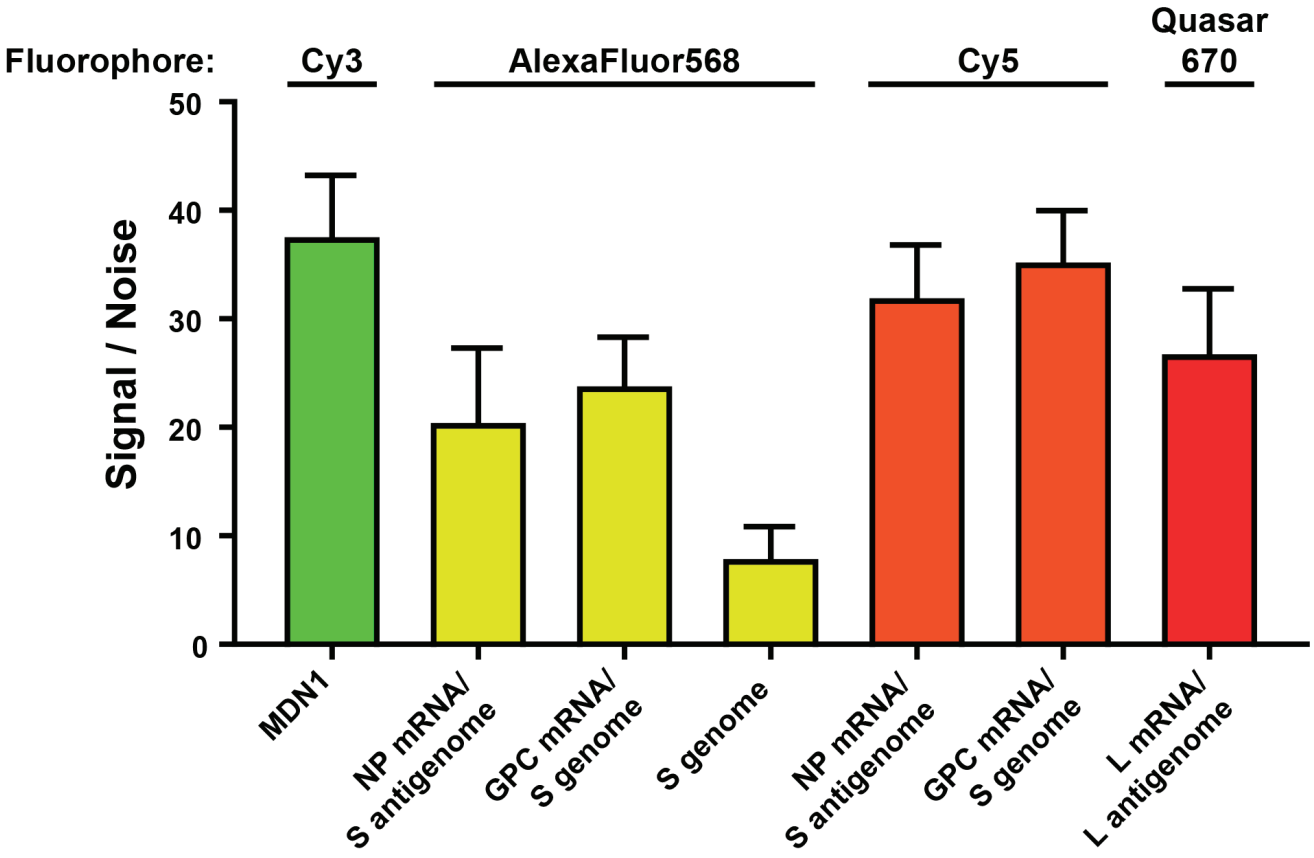
Downloaded from http://jvi.asm.org/ on March 6, 2020 at NYU LANGONE MED CTR-SCH OF MED

Accepted Manuscript Posted Online

Journal of Virology

JVI

Journal of Virology



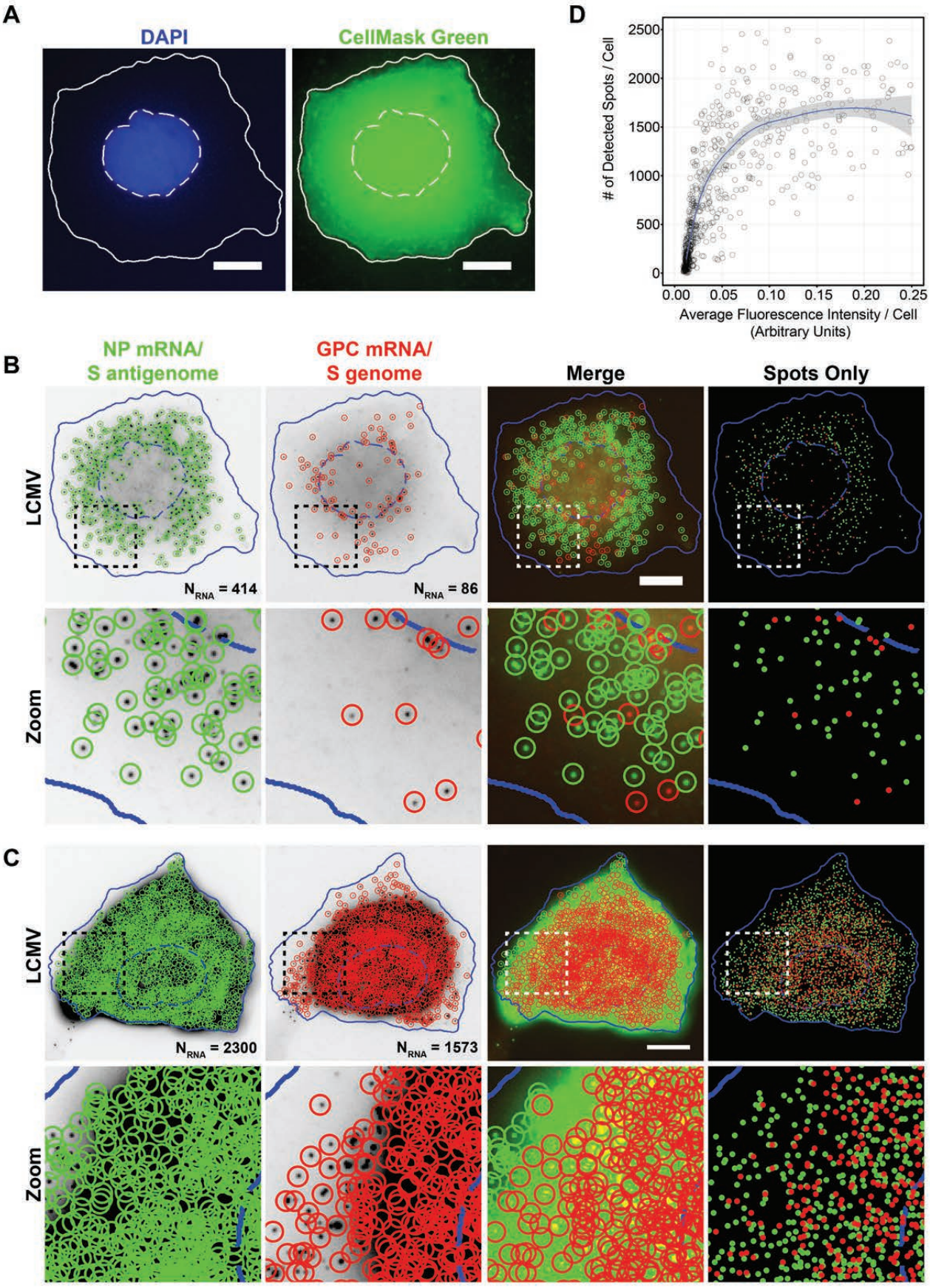
Downloaded from http://jvi.asm.org/ on March 6, 2020 at NYU LANGONE MED CTR-SCH OF MED

Accepted Manuscript Posted Online

Journal of Virology

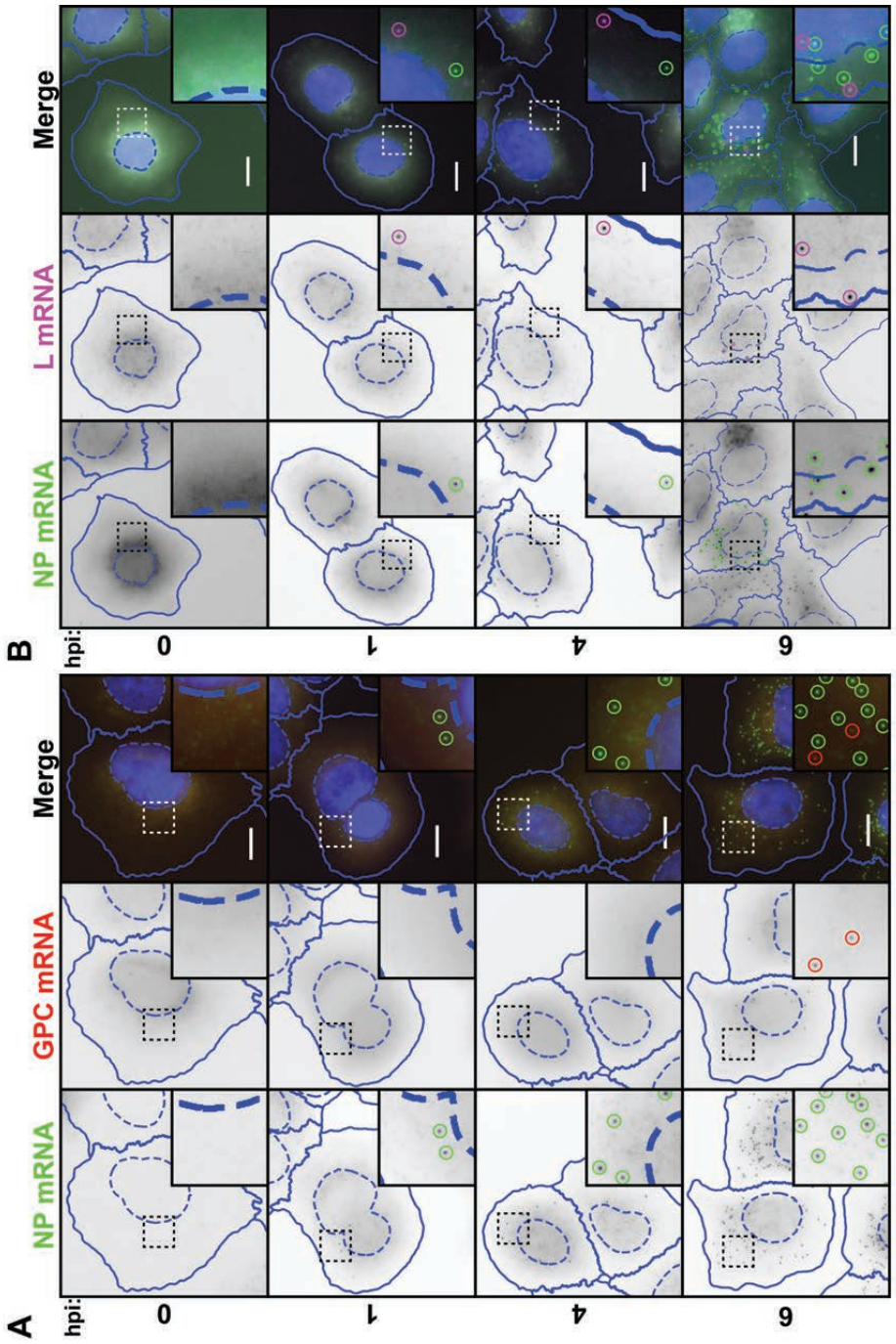
JVI

Journal of Virology



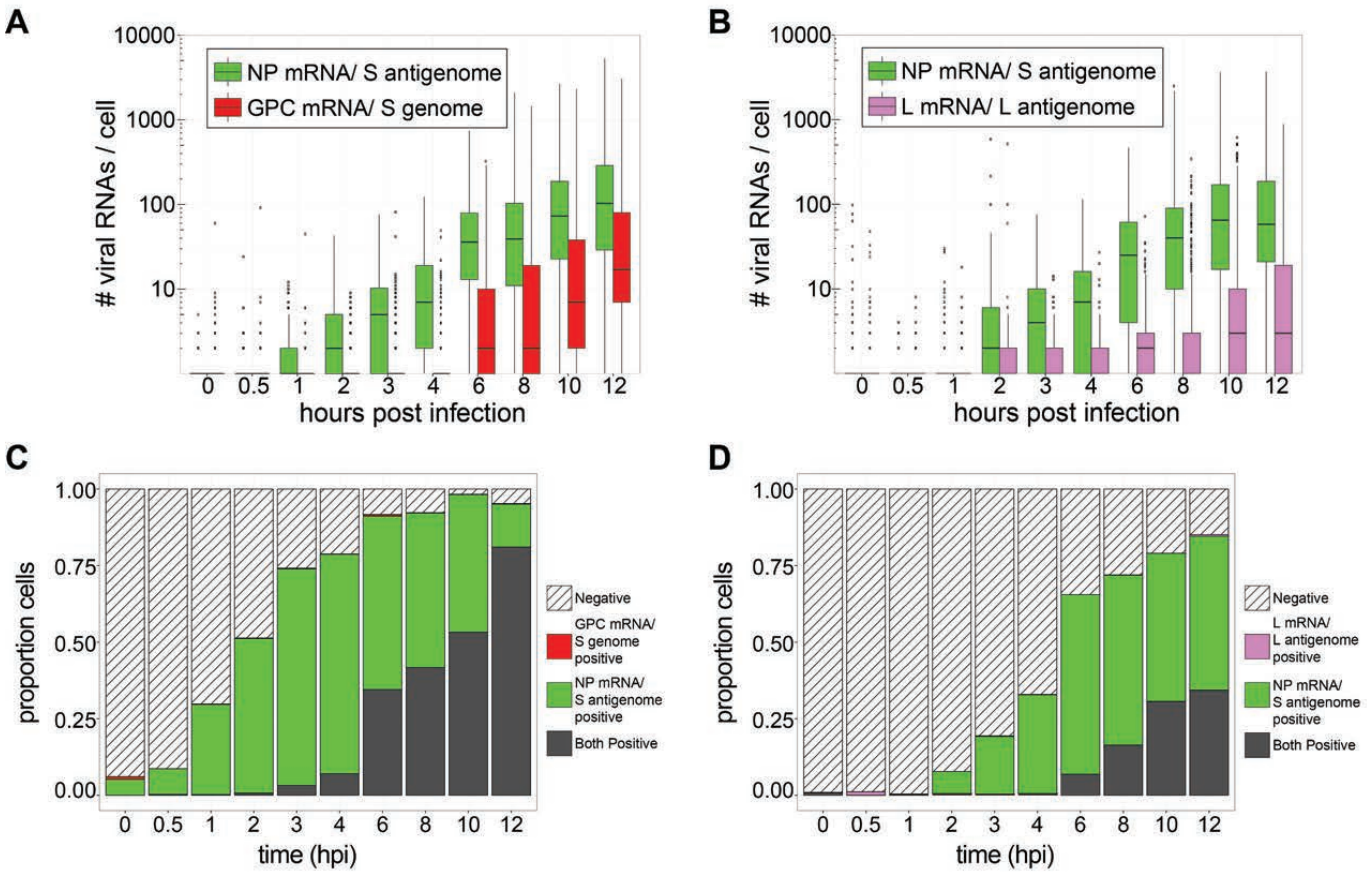
Downloaded from http://jvi.asm.org/ on March 6, 2020 at NYU LANGONE MED CTR-SCH OF MED

Downloaded from http://jvi.asm.org/ on March 6, 2020 at NYU LANGONE MED CTR-SCH OF MED



Accepted Manuscript Posted Online

Accepted Manuscript Posted Online
Journal of Virology
JVI
Journal of Virology



Downloaded from http://jvi.asm.org/ on March 6, 2020 at NYU LANGONE MED CTR-SCH OF MED

Accepted Manuscript Posted Online

Journal of Virology

JVI

Journal of Virology

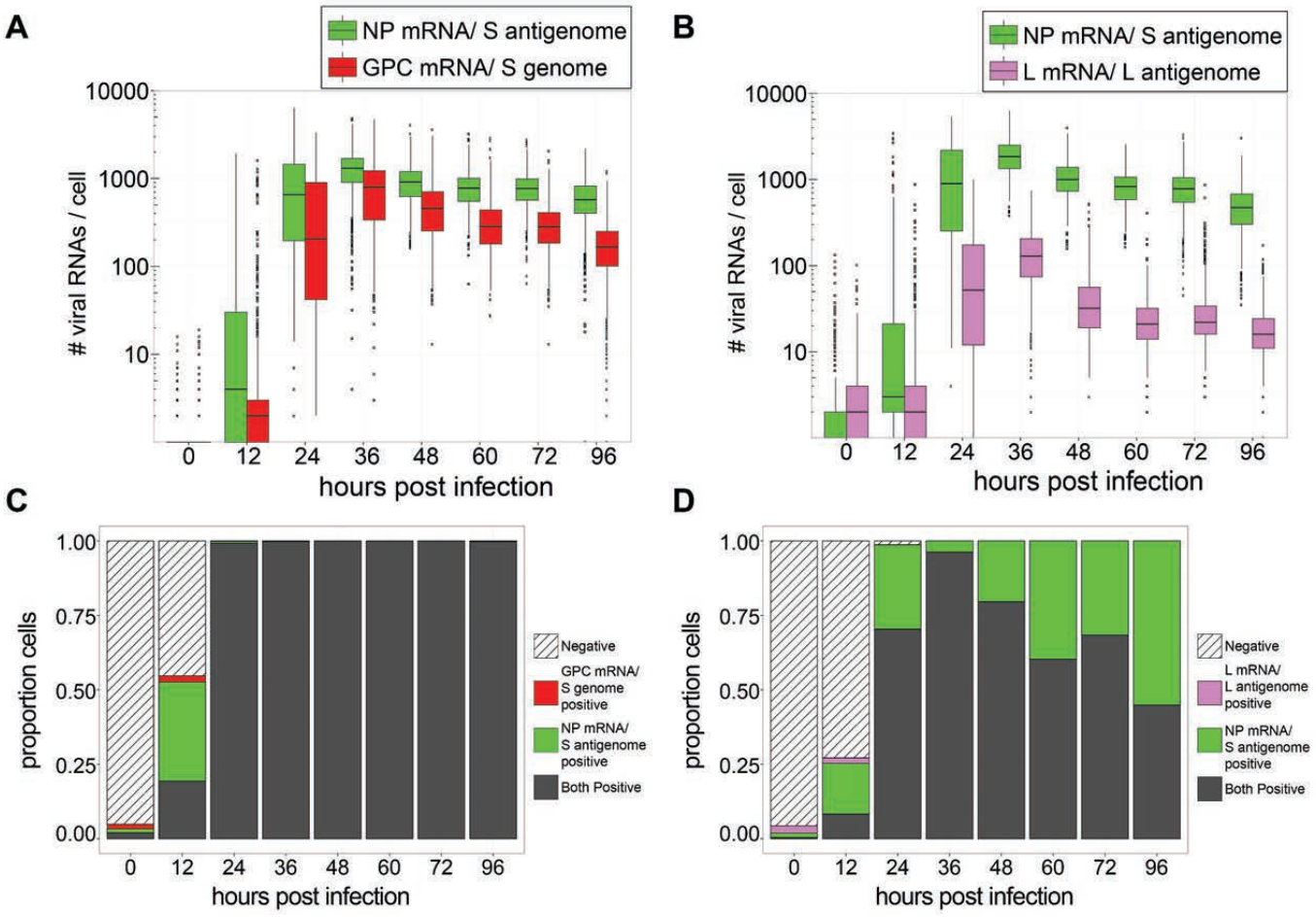
Downloaded from http://jvi.asm.org/ on March 6, 2020 at NYU LANGONE MED CTR-SCH OF MED

Accepted Manuscript Posted Online

Journal of Virology

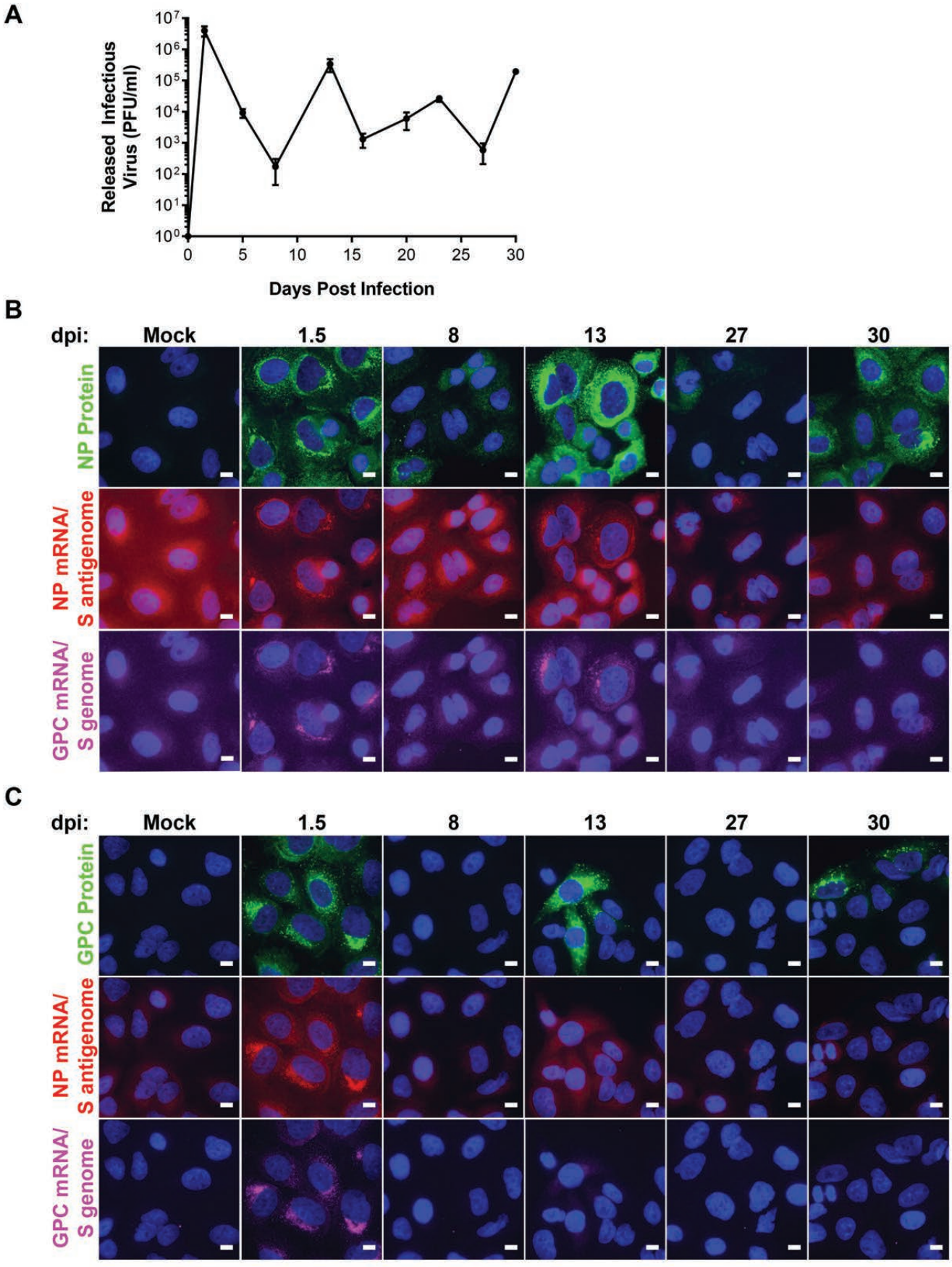
JVI

Journal of Virology



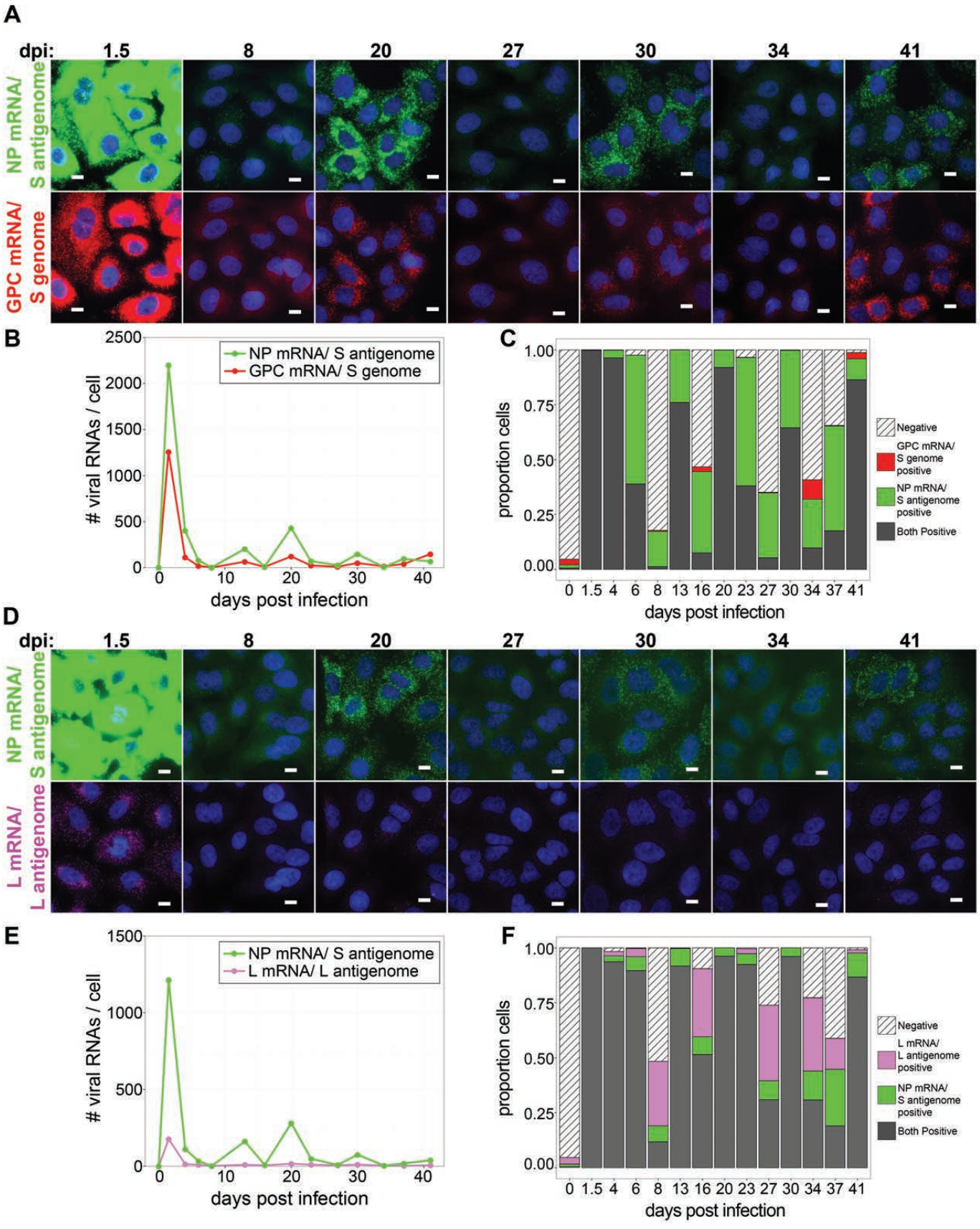
Downloaded from http://jvi.asm.org/ on March 6, 2020 at NYU LANGONE MED CTR-SCH OF MED

Accepted Manuscript Posted Online
Journal of Virology
JVI
Journal of Virology



Downloaded from http://jvi.asm.org/ on March 6, 2020 at NYU LANGONE MED CTR-SCH OF MED

Accepted Manuscript Posted Online



Downloaded from http://jvi.asm.org/ on March 6, 2020 at NYU LANGONE MED CTR-SCH OF MED

Journal of Virology JVI Journal of Virology